Finite temperature phase transitions in non-abelian gauge theories

by

SRINATH CHELUVARAJA

A THESIS IN PHYSICS

Presented to the University of Madras in partial fulfillment of the requirements for the degree of Doctor of Philosophy

July 1996

The Institute of Mathematical Sciences
C.I.T. Campus, Taramani
Madras 600113 INDIA

हिरण्मयेन पात्रेण सत्यस्यापिहितं मुखम ।
तत्त्वं पूषन्नपावृणु सत्यधर्माय दृष्टये ॥

– Isa Upanishad.

The truth is covered by a brilliant golden lid.
May this lid be removed, so that the truth may be seen.

CERTIFICATE

This is to certify that the Ph.D. thesis titled ***Finite temperature phase transitions in non-abelian gauge theories*** submitted by SRINATH CHELUVARAJA is a record of bonafide research work done under my supervision. The research work presented in this thesis has not formed the basis for the award to the candidate of any Degree, Diploma, Associateship, Fellowship or other similar titles. It is further certified that the thesis represents independent work by the candidate and collaboration when existed was necessitated by the nature and scope of the problems dealt with.

H. S. Sharatchandra

Thesis Supervisor

July 1996

Abstract

In this thesis we make a systematic study of the $SO(3)$ lattice gauge theory at finite temperature. Unlike the group $SU(2)$, the group $SO(3)$ has a trivial center subgroup. The center of $SU(2)$ ($Z(2)$) plays an important role in determining the finite temperature properties of the $SU(2)$ lattice gauge theory. Nevertheless, the universality of lattice gauge theory actions suggests that the $SO(3)$ and $SU(2)$ lattice gauge theories (LGTs) have the same continuum limit. Therefore, the study of the $SO(3)$ LGT is important in understanding the implications of lattice gauge theories for the high temperature phase of the $SU(2)$ Yang-Mills theory. A complication present in the $SO(3)$ theory is the existence of a first order bulk transition at zero temperature, which can influence its finite temperature behaviour. A further complication is the presence of a local symmetry, which requires us to use a different set of observables to study its properties. We mainly use the Wilson-Polyakov line in the adjoint representation of $SU(2)$ to make our studies. The role of the $Z(2)$ monopoles in determining the various phases is also considered. We find that the adjoint Wilson line displays an unusual behaviour at low and high temperatures. On the other hand, the fundamental Wilson line is always zero in this model. We analyze the high temperature phase of the theory by looking at the single site histograms for the fundamental and adjoint Wilson lines. We interpret this phase, and draw comparisons with the high temperature phase of the $SU(2)$ LGT theory. We show that the high temperature phase of the $SO(3)$ LGT is like the deconfined phase of the $SU(2)$ LGT theory, though there is no breaking of any symmetry as in the $SU(2)$ theory. We also notice an interference of the bulk transition in the finite temperature theory, as observed in recent studies with mixed action LGTs. One of

the transitions that we observe is a continuation of the zero temperature bulk transition. We study how this transition shifts, as the temperature is increased. We then present evidence for a new phase transition, which is in the region of relevance for the continuum theory. This transition is shown to occur at very low temperatures for the lattices and couplings that we are using. We suggest that this transition is probably a weak first order transition. We then present our conjectured phase diagram for the $SO(3)$ LGT theory at finite temperature and contrast it with that of the $SU(2)$ LGT theory. Finally, we discuss the implications of our results for the high temperature phase of the $SU(2)$ Yang-Mills theory, and argue that it is in the Higgs phase.

To

the imsc1, imsc2 and imsc3 computer systems.

Acknowledgments

It is a pleasure to thank my thesis supervisor H.S.Sharatchandra for his guidance and patience during all these years.

I thank Sundar for his help in the preparation of this manuscript. I also thank Sreedhar and Suryaramana for reading the manuscript and suggesting many improvements.

I am grateful to the members of our institute who are behind the development and maintenance of the computer system, for providing such excellent computational facilities. I thank Hari Dass and Ramesh Anishetty with whom I have had useful discussions on numerous occasions. I also thank the library and administrative staff for their constant assistance.

I would like to thank my parents for their concern and patience. Finally, I would like to thank the friends I made during my stay in Matscience for their lively company, their sense of humour (rather unconventional) and of course for all the storytelling.

Contents

Chapter 1

Introduction

Gauge theories are expected to pass over into new phases at high temperatures. Quantum Chromodynamics (QCD), which is a non-abelian gauge theory of confined quarks and gluons having $SU(3)$ symmetry, may possess a high temperature deconfining phase, in which quarks and gluons can exist as free particles. Apart from its intrinsic theoretical interest, the high temperature properties of QCD may prove useful in explaining several astrophysical and cosmological phenomena, where very high temperatures are known to occur. Recent experiments in heavy ion colliders [1] make it also possible to create these high temperature phases in the laboratory and confront theoretical predictions with experiment. Some of the issues of interest surrounding the high temperature phase are the nature of it's elementary excitations, it's confining or non-confining properties and it's static and dynamic properties.

Though asymptotic freedom [2] requires that the effective coupling constant diminish in strength at high temperatures [3], and therefore makes a perturbative approach possible, infrared divergences appearing at high orders cause the perturbative expansion to diverge[4] and prevent it from being useful in calculating properties dependent on long distance behaviour like the spectrum and the elementary excitations. This requires us to consider non-perturbative methods to study the high temperature phase of QCD. A powerful approach to investigate non-perturbative

phenomena in QCD is to study its properties on a euclidean space time lattice. Lattice gauge theories [5] are finite and defined non-perturbatively at the very outset. Since euclidean field theories can also be regarded as statistical mechanical systems, euclidean lattice gauge theories (LGTs) bear a striking resemblance to statistical mechanical models and allow many known techniques to be used in analyzing their properties. These include series expansions, duality transformations, renormalization group methods and numerical Monte-Carlo methods. Among them, the Monte-Carlo simulation method [6], which has been so effectively used in statistical and condensed matter physics, has proved to be the most versatile.

If lattice gauge theories are to make any predictions for continuum physics, the zero lattice spacing limit must be taken in a sensible way, so as to regain QCD. For asymptotically free gauge theories like QCD, the zero lattice spacing limit is taken in the weak coupling region. Monte-Carlo simulations allow us to approach the weak coupling limit, and hence make predictions for the continuum theory.

Polyakov and Susskind [7] studied the high temperature properties of the pure $SU(2)$ LGT in the strong coupling limit, and showed the existence of a deconfining phase in which static quarks are Debye screened, rather than being confined. In this limit, they showed that the partition function of the $SU(2)$ LGT can be rewritten as a spin model having a global center ($Z(2)$ for $SU(2)$) symmetry, which is spontaneously broken in the high temperature (deconfining) phase. Monte Carlo simulation techniques [8], which can go beyond the the strong coupling limit, also indicate a phase transition into a Debye screened phase. Yaffe and Svetitsky [9] suggested that the critical properties of this transition are similar to those seen in three dimensional spin models having this center($Z(2)$ for $SU(2)$) as the symmetry. There are also some rigorous results [10] for LGTs, which show the existence of a

deconfining phase at high temperatures. Despite these advances, the nature of the high temperature phase of pure gauge theories remains unclear. This is because the magnetic sector is non-perturbative in nature [11]. Though static quarks are Debye screened, the area law behaviour of spatial Wilson loops [12] indicates the presence of non perturbative effects, which prevents the high temperature phase from being considered as an ideal gas of gluons. The elementary excitations of this phase are not known with any certainty.

Most Monte-Carlo studies of LGTs at finite temperature have focused on the Wilson action in their simulations, though mixed actions have also been considered for the $SU(2)$ [13], $SU(3)$ [14] and SU(4) [15] theories. These mixed action LGTs have the same classical continuum limit as LGTs defined using the Wilson action and hence their study can be used to draw conclusions about the features present in the continuum theory. However, mixed action LGTs have several phase transitions at zero temperature, which complicate the study of their finite temperature properties. Since these transitions can often mimic and mask the finite temperature transitions, a careful disentangling of the two is necessary.

Gavai et al [13] considered the finite temperature properties of a mixed action $SU(2)$ LGT, whose action is the sum of the plaquettes in the fundamental and adjoint representations. They studied the Bhanot-Creutz model[16], which is defined as

$$S = \frac{\beta_f}{2} \sum_{n\mu\nu} Tr_f U(n;\mu\nu) + \frac{\beta_a}{3} \sum_{n\mu\nu} Tr_a U(n;\mu\nu).$$

Here Tr_f and Tr_a respectively denote the trace of the plaquette variable $U(n;\mu\nu)$ in the fundamental and adjoint representations, respectively.

They found that the deconfinement transition in this model apparently joined the bulk transition, and were unable to discern any separation between the two. Studies with mixed actions for the group $SU(3)$ [14], have shown a similar merging of the bulk and finite temperature transitions. Various scenarios [13] have been proposed to accommodate these features. If the transitions do indeed merge, the entire line of transitions is either a result of only bulk effects, or only finite temperature effects. It is difficult to reconcile both these possibilities with either theoretical arguments or simulation results. Moreover, it is also possible that the merging is not exact, and that a clear separation between the two transitions occurs only on larger lattices. This would imply the existence of two separate transitions with different properties.

In this thesis, we try to clarify these issues by making a careful study of the finite temperature properties of the Bhanot-Creutz model in the $\beta_f = 0$ limit, which is like studying an $SO(3)$ LGT. Unlike the group $SU(2)$, the group $SO(3)$ has a trivial center subgroup. The center of $SU(2)$ ($Z(2)$) plays an important role in the $SU(2)$ deconfinement transition. Nevertheless, by the universality of lattice gauge theory actions, $SU(2)$ and $SO(3)$ LGTs have the same continuum limit. Hence, one be wonders if the arguments based on the existence of a center symmetry, have any role to play in the continuum limit. Another complication present in the $SO(3)$ LGT is the existence of a zero temperature transition [17], which can possibly effect its finite temperature behaviour. In order to study the finite temperature properties of the $SO(3)$ LGT, we have to consider observables different from the ones used in the study of the $SU(2)$ theory. We mainly consider the Wilson line defined in the adjoint representation of $SU(2)$. By studying its behaviour, we observe phase transitions to a high temperature deconfining phase. We study these transitions and the nature of the high temperature phase. The role of $Z(2)$ monopoles in

determining the phase structure is also studied. We interpret our observations as evidence for the existence of a new phase transition, which is separated from the bulk transition. We then present our conjectured phase diagram for the $SO(3)$ LGT at non zero temperature. Based on our observations, we present a scenario for the high temperature phase and argue that it is in the Higgs phase.

The contents of this thesis are arranged as follows. The second chapter collects together some of the concepts and techniques which we have found useful in examining the aforementioned issues. The third chapter discusses some theoretical properties of order parameters in finite temperature gauge theories. The fourth chapter contains our analysis of the finite temperature properties of the $SO(3)$ LGT. In the final chapter, we discuss our conclusions, and present a scenario for the high temperature phase.

Chapter 2

Basic Concepts

In this chapter we collect together some concepts and techniques which have proved useful in examining the questions raised in this thesis. A brief outline of the finite temperature formalism for non-abelian gauge theories is presented. This is followed by a fairly detailed account of lattice gauge theories, as we have made our studies within that framework. The strong coupling calculation of Polyakov and Susskind, where the existence of a high temperature deconfining phase was first demonstrated, is also presented. The Monte-Carlo technique, along with some of its important results is discussed. Finally, we mention the recent work on mixed lattice gauge theories and their implications for the Yang-Mills theory.

2.1 Finite Temperature Field Theory Formalism

The action for an $SU(2)$ invariant non abelian gauge theory is

$$S = \frac{-1}{2} \int d^4x Tr(F_{\mu\nu}(x) F_{\mu\nu}(x)), \tag{2.1}$$

where $F_{\mu\nu}(x)$ are the field strengths defined by

$$F_{\mu\nu}(x) = \partial_\mu A_\nu(x) - \partial_\nu A_\mu(x) + g[A_\mu(x), A_\nu(x)]. \tag{2.2}$$

The vector potentials $A_\mu(x)$ take values in the Lie algebra of $SU(2)$, and they are expressed as $A_\mu(x) = A^a_\mu(x)\frac{\tau^a}{2}$. The Pauli matrices τ^as satisfy the $SU(2)$

commutation relations

$$[\tau^a/2, \tau^\beta/2] = i\epsilon^{\alpha\beta\gamma}\tau^\gamma/2 \tag{2.3}$$

and are normalized as

$$Tr(\tau^\alpha\tau^\beta) = 2\delta^{\alpha\beta}. \tag{2.4}$$

The vector potentials and field strengths respectively transform under local $SU(2)$ gauge transformations as

$$A_\mu(x) \to V(x)A_\mu(x)V^{-1}(x) - \frac{1}{g}(\partial_\mu V(x))V^{-1}(x), \tag{2.5}$$

$$F_{\mu\nu}(x) \to V(x)F_{\mu\nu}(x)V^{-1}(x), \tag{2.6}$$

where $V(x)$ is an $SU(2)$ matrix.

It is convenient to pass over to the Hamiltonian in the $A_0 = 0$ gauge, where it takes the form

$$H = \frac{1}{2}\int d^3x(E_i^a(\vec{x})E_i^a(\vec{x}) + B_i^a(\vec{x})B_i^a(\vec{x})). \tag{2.7}$$

The field $B_i^a(\vec{x})$ is the non abelian magnetic field and is defined by

$$B_i^a(\vec{x}) = \epsilon_{ijk}\partial_j A_k^a(\vec{x}) + g\epsilon^{\alpha\beta\gamma}A_i^\beta(\vec{x})A_i^\gamma(\vec{x}), \tag{2.8}$$

and $E_i^a(\vec{x})$ is the non abelian electric field, which is the conjugate of $A_i^a(\vec{x})$.

The quantization of this theory proceeds by imposing the canonical commutation relations for the conjugate variables $E_i^a(\vec{x})$ and $A_i^a(\vec{x})$,

$$[E_i^a(\vec{x}), A_j^\beta(\vec{x}')] = -i\delta_{ij}\delta^{ab}\delta(\vec{x} - \vec{x}'). \tag{2.9}$$

The Hamiltonian is invariant under time independent gauge transformations $V(\vec{x})$, which can be parametrized by $V(\vec{x}) = \exp\ i\lambda(\vec{x})$ and $\lambda(\vec{x}) = \lambda^a(\vec{x})\tau^a/2$. These gauge transformations are generated by the operator

$$U_{V(\vec{x})} = \exp\left(i\int d^3x\lambda^a(\vec{x})D_iE_i^a(\vec{x})\right), \tag{2.10}$$

where the covariant derivative of $E_i^a(\vec{x})$ has been defined to be

$$D_i E_i^a(\vec{x}) = \partial_i E_i^a(\vec{x}) + g\epsilon^{a\beta\gamma} A_i^\beta(\vec{x}) E_i^\gamma(\vec{x}). \tag{2.11}$$

Since the Gauss law emerges as a constraint in the quantization process, the physical states must satisfy

$$D_i E_i^a(\vec{x})|\psi\rangle = 0. \tag{2.12}$$

The finite temperature properties are calculated from the partition function

$$Z = Tr'(\exp(-\beta H)), \tag{2.13}$$

where the prime indicates that the trace is taken only over the physical (gauge invariant) states. The operator projecting the states into the physical sector is

$$P = \int D\lambda^a(\vec{x}) \exp\Big(i \int d^4x \lambda^a(\vec{x}) D_i E_i^a(\vec{x})\Big), \tag{2.14}$$

where $D\lambda^a(\vec{x})$ is the $SU(2)$ Haar measure. The partition function in the $|A_i^a(\vec{x})\rangle$ basis is

$$Z = \int DA_i^a(\vec{x}) \langle A_i^a(\vec{x})|P \exp\,(-\beta H)|A_i^a(\vec{x})\rangle. \tag{2.15}$$

The projection operator P ensures that only the physical states appear in the partition function calculation. The partition function can be expressed as a Euclidean path integral propagating in imaginary time x_4 ($x_4 = it$) for a duration $x_4 = i\beta$. Dividing the interval β into N slices of length β/N, the exponential can be written as

$$\exp(-\beta H)P = [\exp(-\beta H/N)P]^N. \tag{2.16}$$

For N large

$$\begin{aligned} \exp(-\beta H/N) &= \exp((-\beta/2N) \int d^3x E_i^a(\vec{x}) E_i^a(\vec{x})) \\ & \exp((-\beta/2N) \int d^3x B_i^a(\vec{x}) B_i^a(\vec{x})). \end{aligned} \tag{2.17}$$

Inserting a complete set of states $|A_i^a(x)\rangle\langle A_i^a(x)|$ and $|E_i^a(x)\rangle\langle E_i^a(x)|$ for each time slice, we obtain

$$\begin{aligned} Z &= \int_{pbc} D\lambda^a(x) DA_i^a(x) DE_i^a(x) \\ &\exp\Big(\int_0^\beta dx_4 \int d^3x (i\ E_i^a(x)\dot{A}_i^a(x) - (\frac{1}{2}E_i^a(x)E_i^a(x) + \frac{1}{2}B_i^a(x)B_i^a(x)))\Big) \\ &\exp\Big(i\ \int_0^\beta dx_4 \int d^3x \lambda^a(x) D_i E_i^a(x)\Big). \end{aligned} \tag{2.18}$$

Since we are taking the trace, the $A_i^a(x)$ fields in the path integral are periodic in time with period β (this is indicated by the subscript pbc). Integration over the $E_i^a(x)$ fields gives

$$\begin{aligned} Z &= \int_{pbc} D\lambda^a(x) DA_i^a(x) \\ &\exp\Big(\frac{-1}{2}\int_0^\beta dx_4 \int d^3x [(\dot{A}_i^a(x) - D_i\lambda^a(x))^2 + B_i^a(x)B_i^a(x)]\Big) \end{aligned} \tag{2.19}$$

The integration is over fields periodic in the time direction with period β. Renaming the $\lambda^a(x)$ field as $A_4^a(x)$, the partition function becomes

$$Z = \int_{pbc} [DA_\mu] \exp(-S_E), \tag{2.20}$$

where S_E is the Euclidean Yang-Mills action,

$$S_E = \frac{1}{2}\int d^3x dx_4 Tr(F_{\mu\nu}(x)F_{\mu\nu}(x)). \tag{2.21}$$

Therefore, the partition function calculation reduces to the Euclidean path integral over all field configurations which are periodic in time with period β.

The periodicity in the time direction allows us to define the gauge invariant observable called the Wilson-Polyakov line. It is defined as

$$L_f(\vec{x}) = Tr\ P \exp\Big(ig\int_0^\beta dx_4 A_4^a(\vec{x}, x_4)\tau^a/2\Big), \tag{2.22}$$

where f denotes the trace in the fundamental representation of $SU(2)$. It can be regarded as measuring the amplitude for a static quark (defined in the fundamental representation of $SU(2)$) to propagate in a heat bath of temperature β^{-1}. The expectation value of this observable is given by

$$\langle L_f(\vec{x})\rangle = \frac{Z[L_f(\vec{x})]}{Z}, \tag{2.23}$$

where $Z[L_f(\vec{x})]$ is

$$Z[L_f(\vec{x})] = \int [DA_\mu] \exp(-S_E)\, Tr\ P \exp\ \left(ig \int_0^\beta dx_4 A_4^a(\vec{x}, x_4)\tau^a/2 \right). \tag{2.24}$$

It can be given a physical interpretation by writing Z and $Z[L_f(\vec{x})]$ as the exponential of a free energy, $Z = \exp(-\beta F(0))$ and $Z[L_f(\vec{x})] = \exp(-\beta F_f(\vec{x}))$. The Wilson line expectation value can be written as

$$\langle L_f(\vec{x})\rangle = \exp\Big(-\beta[F_f(\vec{x}) - F(0)]\Big). \tag{2.25}$$

Written in this way, it measures the difference in free energy of a single quark state (at $\vec{x}$) and the vacuum, in a heat bath of temperature β^{-1}. The correlation function between two Wilson lines can be similarly expressed as

$$\langle L_f(\vec{x}) L_f(\vec{y})\rangle = \exp\Big(-\beta[F_f(\vec{x} - \vec{y}) - F(0)]\Big). \tag{2.26}$$

It measures the difference in free energy of a static quark anti-quark pair located at the points $\vec{x}$ and $\vec{y}$, and the vacuum. This free energy is nothing but the quark-antiquark potential (including self energy effects) in a heat bath of temperature β. Under $SU(2)$ gauge transformations, the Wilson-Polyakov line (henceforth called the Wilson line) transforms as

$$L_f(\vec{x}) \to Tr\ \left(V(\vec{x}, 0)\ P\ \exp\ (ig \int_0^\beta dx_4 A_4^a(\vec{x}\, x_4)\tau^a/2)\ V^\dagger(\vec{x}, \beta) \right), \tag{2.27}$$

where $V(x)$ is an $SU(2)$ matrix. Hence, $L_f(\vec{x})$ is invariant under periodic gauge transformations $V(\vec{x},\beta) = V(0,\beta)$.

The finite temperature euclidean path integral has a larger symmetry, owing to the periodic boundary conditions in the time direction. Gauge transformations which are periodic up to an element of the center of the group, are also symmetries of the action [9]. Let

$$V(\vec{x}, x_4 + \beta) = ZV(\vec{x}, x_4), \tag{2.28}$$

where Z is an element of the center of $SU(2)$. The center of $SU(2)$ consists of the elements $+1$ and -1, since these are the only elements which commute with all the members of the group. These gauge transformations leave the gauge fields unchanged, as can be seen from Eq. 2.5 and the fact that $ZA_i(x)Z^{-1} = A_i(x)$. Hence, they are additional symmetries of the action. Local observables are invariant under these aperiodic gauge transformations, but the Wilson line transforms as

$$L_f(\vec{x}) \rightarrow ZL_f(\vec{x}). \tag{2.29}$$

Nevertheless, the correlation function of Wilson lines is invariant under this transformation.

If $\langle L_f(\vec{x})\rangle \neq 0$, then this center symmetry is spontaneously broken and $F(L_f(\vec{x}))$ is finite (see Eq. 2.25). This implies that static quarks have finite energy and the theory is in the deconfined phase. The center symmetry implies that the Wilson line will take two values related by a $Z(2)$ transformation. The correlation functions in this phase behave as

$$\langle L_f^\dagger(\vec{x})L_f(\vec{0})\rangle = |\langle L_f(\vec{0})\rangle|^2(1 + \beta e^2 \frac{\exp -|\vec{x}|\mu}{|\vec{x}|^p}), \tag{2.30}$$

giving a short range potential (see Eq. 2.26) between quarks. In the absence of spontaneous symmetry breaking, $\langle L_f(\vec{x})\rangle = 0$ and from Eq. 2.25 $F(L_f(\vec{x})) = \infty$,

implying confinement of static quarks. The correlation functions in the unbroken phase decay exponentially as

$$\langle L_f^\dagger(\vec{x}) L_f(\vec{0}) \rangle = \exp(-\sigma\beta|\vec{x}|), \tag{2.31}$$

yielding a linear confining potential (see Eq. 2.26) between static quarks, with a string tension σ.

The behaviour of the Wilson line distinguishes the confining and deconfining phases, and hence it can serve as an order parameter to study the phase transition at high temperatures. We note that the low temperature confining phase corresponds to the disordering of the Wilson lines (since $\langle L_f(\vec{x}) \rangle = 0$), while the high temperature deconfining phase corresponds to the ordering of the Wilson lines (since $\langle L_f(\vec{x}) \rangle \neq 0$). This is in contrast to the situation familiar in statistical mechanical systems, where the ordering is present at low temperatures and disappears at high temperatures. Thus, $L_f(\vec{x})$ is like a disorder variable rather than an order parameter.

Another observable whose behaviour can be studied across the transition is the spatial Wilson loop. However, it is not very sensitive to the phase transition and

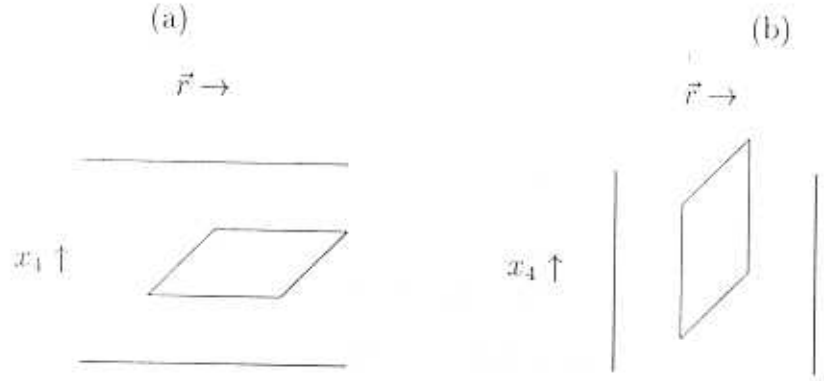

displays an area law behaviour at all temperatures. It is natural to expect an area law behaviour at low temperatures, since the zero temperature theory is confining. That the same also holds true at high temperatures can be seen by the following qualitative argument [9]. The figure (a) above shows a spatial Wilson loop at some large temperature β^{-1}. By relabelling the time axis as a space axis and one of the space axes as the time axis, it can equally well be considered as a temporal Wilson loop at zero temperature, but in a volume which is finite in one direction (see (b)) with periodic boundary conditions. Temporal Wilson loops have an area law behaviour at low temperatures because the zero temperature theory is confining, and enclosing them in finite volumes does not alter this property. This results in an area law behaviour at all temperatures. There are also rigorous arguments [27] which arrive at the same conclusion.

Since the spatial degrees of freedom are unaffected by the transition, they can be integrated out to get an effective three dimensional theory of Wilson lines. This effective three dimensional theory resembles some well known spin models, which also have the same global center symmetry. Svetitsky and Yaffe [9] suggested that the critical properties of the transition could be understood as a consequence of the fixed point behaviour of these three dimensional spin models. Depending on the manner in which $\langle L_f(\vec{x}) \rangle$ changes from its zero value in the confining phase to its non zero value in the deconfining phase, the transition is of first, second or higher order.

Asymptotic freedom decrees that the effective coupling constant $g(T) \to 0$ at high temperatures[3]. Nevertheless, this does not allow a perturbative calculation of thermodynamic quantities at high temperatures, because of the infrared divergences which start appearing at higher orders[4]. In order to get a complete understanding

of the properties of the high temperature phase, we have to resort to non perturbative methods of analysis. In the next section we describe the lattice approach to studying the high temperature properties of non abelian gauge theories.

2.2 Gauge Theories on the Lattice

Lattice gauge theories [5] offer a non-perturbative definition of gauge theories and provide a powerful framework for studying their properties. In this section we present the rudiments of lattice gauge theories and explain how they can be related to Yang-Mills theories.

The space time continuum is replaced by a four dimensional hypercubic euclidean lattice, with some lattice spacing a. Gauge fields are defined on the links of this lattice. Every link is labelled by one of its ends n and a direction μ. The site index n denotes a four dimensional vector with spatial components $n1, n2, n3$ and temporal component $n4$. $(n;\mu)$ labels a link beginning from n and pointing in the μ direction while $(n+\mu;-\mu)$ labels the same link but with opposite orientation. On every link, one places a unitary matrix U belonging to the gauge group (in our case $SU(2)$) in question. The variables defined for the two orientations of a single link are related by

$$U(n;\mu) = U^{\dagger}(n+\mu;-\mu). \tag{2.32}$$

These link variables transform under gauge transformations as

$$U(n;\mu) \rightarrow V(n)U(n;\mu)V^{\dagger}(n+\mu), \tag{2.33}$$

where $V(n)$ is an $SU(2)$ matrix. The form of the action on the lattice is chosen such that it is gauge invariant and reproduces the Yang-Mills action when the lattice

spacing a goes to zero. Wilson considered the following action for the pure gauge theory

$$S = \frac{-\beta_f}{2} \sum_{n\mu\nu} Tr_f U(n;\mu\nu), \tag{2.34}$$

where $U(n;\mu\nu)$ are plaquette variables defined by

$$U(n;\mu\nu) = U(n;\mu)U(n+\mu;\nu)U^\dagger(n+\nu;\mu)U^\dagger(n;\nu) \tag{2.35}$$

and the subscript f denotes the trace in the fundamental representation of $SU(2)$. The summation is over all plaquette variables. The plaquette variables $U(n;\mu\nu)$ are so called because they are formed by taking a product of link variables over an elementary square or plaquette. Under gauge transformations, the plaquette variables transform as

$$U(n;\mu\nu) \to V(n)U(n;\mu\nu)V^\dagger(n). \tag{2.36}$$

By the cyclicity of the trace, the action is gauge invariant. One recovers the continuum Yang-Mills action by taking the lattice spacing a to zero. To see this, define

$$U(n;\mu) = \exp\Big(iag\tau^a A^a_\mu(n)/2\Big) \tag{2.37}$$

where $A^a_\mu(n)$ are the continuum gauge fields and g is the coupling constant. The plaquette variables can be written in terms of these fields as

$$\begin{aligned} U(n;\mu\nu) \;=\; & \exp(iag\tau^a A^a_\mu(n)/2)\exp(iag\tau^a A^a_\nu(n+\mu)/2) \\ & \exp(-iag\tau^a A^a_\mu(n+\nu)/2)\exp(-iag\tau^a A^a_\nu(n)/2). \end{aligned} \tag{2.38}$$

Using the Baker-Campbell-Hausdorff (BCH) formula

$$\exp A \exp B = \exp(A+B) + 1/2[A,B] + 1/12[[A,B],B] + \ldots \quad , \tag{2.39}$$

we have

$$U(n;\mu\nu) = \exp\Big(iag\tau^a/2(A^a_\mu(n) + a\partial_\mu A_\nu(n) + A^a_\nu(n) + O(a^2))\Big)$$
$$\exp\Big(-iag\tau^a/2(A^a_\mu(n) + a\partial_\nu A_\mu(n) + A^a_\nu(n) + O(a^2))\Big) \quad (2.40)$$

Again using the BCH formula for combining the exponentials, we get

$$U(n;\mu\nu) = \exp\Big(ia^2 g\tau^a/2(\partial_\mu A^a_\nu(n) - \partial_\nu A^a_\mu(n) + g\epsilon^{\alpha\beta\gamma}A^\beta_\mu(n)A^\gamma_\nu(n) + O(a))\Big), \quad (2.41)$$

where the plaquette variables are seen to be directly related to the field strengths as

$$U(n;\mu\nu) = \exp\ (ia^2 g\tau^a F^a_{\mu\nu}(n)/2 + O(a^3)). \quad (2.42)$$

In the limit of zero lattice spacing

$$U(n;\mu\nu) = 1 + ia^2 g\tau^a F^a_{\mu\nu}(n)/2 - a^4 g^2/2(\tau^a F^a_{\mu\nu}(n)/2)(\tau^a F^a_{\mu\nu}(n)/2) + .. \quad (2.43)$$

and the action becomes

$$\frac{-\beta_f}{2}\sum_{n\mu\nu} Tr\ U(n;\mu\nu) = \frac{\beta_f g^2}{8}\int d^4x\ Tr(F_{\mu\nu}(x)F_{\mu\nu}(x)). \quad (2.44)$$

The further factor of half comes from the antisymmetry of $F_{\mu\nu}(x)$. The summation over all plaquettes has been replaced by an integral as

$$a^4\sum_{n\mu\nu} \to \int d^4x \quad (2.45)$$

and the terms of higher order in a vanish in the zero lattice spacing limit. Choosing $\beta_f = 4/g^2$, we regain the (Euclidean) Yang-Mills action.

$$S_E = \frac{1}{2}\int d^4x Tr(F_{\mu\nu}(x)F_{\mu\nu}(x)). \quad (2.46)$$

The above method of taking the zero lattice spacing limit is called the classical (or naive) continuum limit, because it ignores the effect of quantum corrections.

The gauge invariant observables of the lattice theory are traces of product of link variables over closed loops on the lattice, and they are defined as

$$W(C) = Tr \prod_{l \in C} U(l). \tag{2.47}$$

The behaviour of these Wilson loops is indicative of the various phases of this model. For example, an area law behaviour

$$W(C) = \exp(-\sigma A), \tag{2.48}$$

where A is the area enclosed by the Wilson loop, implies confinement of static quarks with σ as the string tension. A perimeter law behaviour

$$W(C) = \exp(-\alpha L), \tag{2.49}$$

where L is the perimeter of the Wilson loop, indicates a Coulomb or Higgs phase.

For lattice gauge theories to make any predictions about continuum physics, one must be able to take the zero lattice spacing limit and obtain finite and meaningful results. This requires us to also vary β_f as we take $a \to 0$, so that physical quantities like the string tension (σ) remain finite. The string tension on the lattice has the form

$$\sigma = \frac{1}{a^2} f(g). \tag{2.50}$$

For σ to remain finite as $a \to 0$, the function $f(g)$ must also approach zero. This requires us to also vary g, so that $f(g)$ tends to zero. The joint variation of g and a to yield a finite σ, leads to the following renormalization group equation for f

$$-f(g) + \beta(g)\frac{\partial f}{\partial g} = 0, \tag{2.51}$$

where the beta function $\beta(g)$ has been defined as

$$\beta(g) = -a\frac{\partial g}{\partial a}. \tag{2.52}$$

For non abelian gauge theories, the perturbative result valid for weak coupling is

$$\beta(g) = -\beta_0 g^3 - \beta_1 g^5 + O(g^7), \tag{2.53}$$

with β_0 and β_1 as the leading coefficients of the beta function. The negative sign of the beta function forces $g(a) \to 0$ as $a \to 0$. This means that the continuum limit of non abelian lattice gauge theories is in the region $g = 0$ ($\beta_f = \infty$). On solving the renormalization group equation, the form of $f(g)$ turns out to be

$$f(g) = const\ g^{\frac{-\beta_1}{\beta_0^2}} \exp\left(\frac{-1}{2\beta_0 g^2}\right)(1 + O(g)). \tag{2.54}$$

The function $f(g)$ fixes the functional form of the observables which remain finite in the continuum limit. It is also called the scaling function [21] because it determines how physical quantities must behave as a function of g (or β_f) so that they attain finite values in the continuum limit.

The lattice action is not unique, because several gauge invariant constructions can be made which reduce to the Yang-Mills theory in the naive zero lattice spacing limit. Hence we can consider generalizations of the Wilson action, and study their properties. An example which will be relevant for this thesis is the adjoint Wilson action. This is defined as

$$S = \frac{-\beta_a}{3} \sum_{n\mu\nu} Tr_a U(n;\mu\nu), \tag{2.55}$$

where $U(n;\mu\nu)$ are the usual plaquette variables and the subscript a denotes the trace in the adjoint representation of $SU(2)$. The trace in the adjoint representation is related to the trace in the fundamental representation by

$$Tr_a U = (Tr_f U)^2 - 1. \tag{2.56}$$

We can take the naive continuum limit of this model as we did for the fundamental Wilson action. Proceeding as before, and using Eq. 2.56 we get

$$Tr_a U(n;\mu\nu) = \left(2 - (a^4 g^2/2)(\tau^a F^a_{\mu\nu}(n)/2)(\tau^a F^a_{\mu\nu}(n)/2) + ...\right)^2 - 1. \qquad (2.57)$$

The action becomes

$$\frac{-\beta_a}{3}\sum_{n\mu\nu} Tr\ U(n;\mu\nu) = \frac{2\beta_a g^2}{6}\int d^4x\ Tr(F_{\mu\nu}(x)F_{\mu\nu}(x)), \qquad (2.58)$$

after neglecting terms of higher order in a. Comparing Eq. 2.58 and Eq. 2.44 we get the relation

$$\beta_f = \frac{8\beta_a}{3}. \qquad (2.59)$$

This relation holds true only in the naive zero lattice spacing limit. The issue of the continuum limit can also be addressed for this action, as we did for the fundamental Wilson action. It is an important matter to decide whether the two actions lead to the same continuum theory.

The lattice formulation can readily be applied to study gauge theories at finite temperature. The temporal extent of the lattice is chosen to be finite, and periodic boundary conditions are imposed in the time direction. In practice, one works on a lattice whose spatial extent N_σ is much larger than its temporal extent N_τ. The lattice temperature is determined by

$$\beta = N_\tau a. \qquad (2.60)$$

Note that the lattice temperature can be increased by decreasing N_τ at a fixed lattice spacing a or decreasing a at a fixed N_τ. The lattice spacing a can be increased (decreased) by decreasing (increasing) β_f. This follows from the form of the function f and Eq. 2.50. In our studies, we will use both these methods of changing the

temperature on the lattice. The Wilson line can be expressed in terms of the link variables as

$$L_f(\vec{n}) = Tr_f \prod_{n_4=0}^{N_\tau} U(\vec{n} + n_4\hat{4}; \hat{4}). \tag{2.61}$$

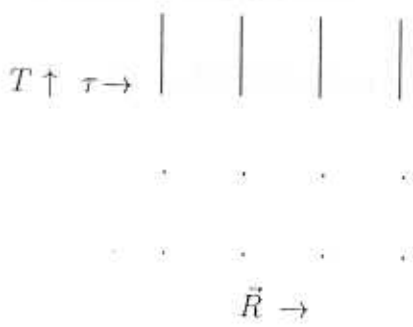

The global center symmetry is the invariance of the action under gauge transformations which are periodic up to a center element. This is equivalent to multiplying all the time like links emanating from some time slice by a center element as shown above. Under this transformation, the Wilson line picks up a center element

$$L_f(\vec{n}) \rightarrow Z L_f(\vec{n}). \tag{2.62}$$

The continuum limit of finite temperature lattice gauge theories would also require the physical temperature to remain finite. This entails taking the limit $N_\tau \rightarrow \infty$ in addition to $a \rightarrow 0$. The physical temperature β_{phys} is given by

$$\beta_{phys} = \lim_{\substack{a \rightarrow 0 \\ N_\tau \rightarrow \infty}} N_\tau a. \tag{2.63}$$

Using Eq. 2.50 and Eq. 2.54 to express the lattice spacing as a function of g, we get

$$g(N_\tau) = \frac{1}{\beta_0 \log(\frac{N_\tau}{\sigma \beta_{cr}^2})}. \tag{2.64}$$

The continuum limit of the lattice theory is achieved by varying g as above and taking $N_\tau \rightarrow \infty$. Since the limit $N_\tau \rightarrow \infty$ cannot be taken in practice, one studies the behaviour of quantities as a function of N_τ.

2.3 Strong Coupling Limit

It is also possible to have a Hamiltonian formulation for lattice gauge theories. Since the calculation of Polyakov and Susskind was performed in this formulation, we describe it in some detail. We will use this later on in this thesis.

The lattice Hamiltonian is a discretized version of the continuum one, and in the $A_0 = 0$ gauge has the form

$$H = (g^2/2a)\sum_{\vec{n}\ i} E^a(\vec{n}\ i)E^a(\vec{n}\ i) + (1/2g^2)\sum_{\vec{n}\ i}(Tr\ U(\vec{n};i\ j) + Tr\ U^\dagger(\vec{n};i\ j)), \quad (2.65)$$

where $E^a(\vec{n}\ i)$ are the non-abelian electric fluxes and $U(\vec{n};ij)$ are the plaquette variables. At the ends of each link, we define the operators $E^a_-(\vec{n}\ i)$ and $E^a_+(\vec{n}\ i)$ which generate left and right gauge transformations on the link variables $U(\vec{n};i)$. The degrees of freedom of an $SU(2)$ LGT are similar to those of an assembly of coupled rotators[20]. $E^a_-(\vec{n}\ i)$ and $E^a_+(\vec{n}\ i)$ are like the angular momentum operators of a spherical top in the space fixed and body fixed axes respectively. The first term in the Hamiltonian is the kinetic energy of the tops, which is the same when expressed in the space fixed or body fixed reference frames,

$$E^a_-(\vec{n}\ i)E^a_-(\vec{n}\ i) = E^a_+(\vec{n}\ i)E^a_+(\vec{n}\ i) = E^a(\vec{n}\ i)E^a(\vec{n}\ i), \quad (2.66)$$

while the second term describes the interactions between the different tops. The operators obey the $SU(2)$ commutation relations

$$[E^a_+(\vec{n}\ i), E^\beta_+(\vec{n}\ i)] = \epsilon^{\alpha\beta\gamma}E^\gamma_+(\vec{n}\ i), \quad (2.67)$$

$$[E^a_-(\vec{n}\ i), E^\beta_-(\vec{n}\ i)] = \epsilon^{\alpha\beta\gamma}E^\gamma_-(\vec{n}\ i), \quad (2.68)$$

$$[E^a(\vec{n}\ i)E^a(\vec{n}\ i), E^a_-(\vec{n}\ i)] = 0, \quad (2.69)$$

$$[E^a(\vec{n}\ i)E^a(\vec{n}\ i), E^a_+(\vec{n}\ i)] = 0. \quad (2.70)$$

A gauge invariant basis for the Hamiltonian is labelled by the simultaneous eigenvectors of $E^a(\vec{n}\ i)E^a(\vec{n}\ i), E^a_-(\vec{n}\ i)$ and $E^a_+(\vec{n}\ i)$ of all the links, and is written as $|j(\vec{n}\ i)\ m(\vec{n}\ i)\ m'(\vec{n}\ i))$, where

$$E^a E^a|j\ m\ m'\rangle = j(j+1)|j\ m\ m'\rangle, \tag{2.71}$$

$$E^a_-|j\ m\ m'\rangle = m|j\ m\ m'\rangle, \tag{2.72}$$

$$E^a_+|j\ m\ m'\rangle = m'|j\ m\ m'\rangle. \tag{2.73}$$

The physical states of the theory are those which satisfy the Gauss law constraint

$$\left(\sum_i E^a_-(\vec{n}\ i) + \sum_i E^a_+(\vec{n}-i\ i)\right)|\psi\rangle = 0, \tag{2.74}$$

which enforces conservation of electric flux at every site.

We now present the strong coupling calculation of Polyakov and Susskind [7], where the existence of a high temperature deconfining phase was first demonstrated. In this limit, the partition function for the $SU(2)$ Yang-Mills theory can be rewritten as that of a spin system having a global center ($Z(2)$) symmetry. In the strong coupling limit ($g \to \infty$), the kinetic term dominates over the potential term and the Hamiltonian is simply

$$H = \frac{g^2}{2a}\sum_{\vec{n}\ i} E^a(\vec{n}\ i)E^a(\vec{n}\ i). \tag{2.75}$$

The partition function is

$$Z = Tr' \exp(-\beta H), \tag{2.76}$$

where the prime indicates that the trace is to be carried out only over the physical states satisfying the Gauss law constraint. The projection operator which imposes this constraint at every site is

$$P(\vec{n}) = \int d\vec{l} \exp\left(il^a\left[\sum_i (E^a_-(\vec{n}\ i) + E^a_+(\vec{n}-i\ i))\right]\right), \tag{2.77}$$

where $d\vec{l}$ is the $SU(2)$ Haar measure.

The partition function is

$$Z = Tr \prod_{\vec{n}\ i} \exp\left((-\beta g^2/2a) E^a(\vec{n}\ i) E^a(\vec{n}\ i)\right) \prod_{\vec{n}} P(\vec{n}). \tag{2.78}$$

It can be rewritten as

$$Z = Tr \int d\vec{l}(\vec{n}) \prod_{\vec{n}\ i} \exp\left(-\frac{\beta g^2 \vec{E}(\vec{n}\ i)^2}{2a} - \vec{l}(\vec{n}).\vec{E}_-(\vec{n}\ i) - i\vec{l}(\vec{n}+i).\vec{E}_+(\vec{n}\ i)\right), \tag{2.79}$$

where we have used the vector notation for l^a, $E^a_-(\vec{n}\ i)$ and $E^a_+(\vec{n}\ i)$. Calculating the trace with respect to the basis states at a particular link, we have

$$\sum_{j,a,b} \langle j;a;b| \exp\left(-\frac{\beta g^2 \vec{E}^2}{2a} - i\vec{l}\vec{E} - i\vec{l}'.\vec{E}\right) |j;a;b\rangle. \tag{2.80}$$

Using Eq. 2.71-2.73 this becomes

$$\sum_{j=0}^{\infty} \exp(-\frac{\beta g^2 j(j+1)}{2a}) \chi_j(\vec{l}) \chi_j(\vec{l}'), \tag{2.81}$$

where the summation is over all half integral values of j. $\chi_j(\vec{l}) = Tr\ \exp(i\vec{l}.T_j)$ and is given by the formula

$$\chi_j(\vec{l}) = \frac{\sin((j+1/2)l)}{\sin(l/2)}, \tag{2.82}$$

where l is the magnitude of the vector $\vec{l}$. l takes values from 0 to 2π. The sum over a single link can be written as

$$\frac{1}{\sin(l/2)\sin(l'/2)} \sum_{j=0}^{\infty} \exp(\frac{-\beta g^2 j(j+1)}{2a}) \sin((j+1/2)l) \sin((j+1/2)l'). \tag{2.83}$$

Here l and l' are the angular variables at the two ends of a link. This summation can be performed using

$$\sum_{E=-\infty}^{\infty} \exp(-cE^2 + i\alpha E) = \sqrt{\left(\frac{\pi}{c}\right)} \exp\left(-\left(\frac{\alpha^2}{4c}\right)\right), \tag{2.84}$$

where the periodic Gaussian function is defined as

$$\tilde{\exp}(-\gamma\phi^2) = \sum_m \exp -\gamma(\phi + 2\pi m)^2. \tag{2.85}$$

The partition function is a product of such terms over all links and can be written as

$$Z = \int_0^{2\pi} \prod_{\vec{n}} dl(\vec{n}) \sin^2\left(\frac{l(\vec{n})}{2}\right) \prod_{\vec{n}\ i} \frac{F(l(\vec{n}) + l(\vec{n}+i), l(\vec{n}) - l(\vec{n}+i))}{\sin\left(\frac{l(\vec{n})}{2}\right) \sin\left(\frac{l(\vec{n}+i)}{2}\right)}) \tag{2.86}$$

and the function F is defined as

$$F(l+l'; l-l') = -\tilde{\exp}\Big[\frac{a}{2\beta g^2}\left(\frac{l+l'}{2}\right)^2\Big] + \tilde{\exp}\Big[\frac{a}{2\beta g^2}\left(\frac{l-l'}{2}\right)^2\Big]. \tag{2.87}$$

The function $F(l+l'; l-l')$ has the following properties. It is periodic in $l+l'$ and $l-l'$ with period 4π and is antisymmetric under exchange of $l+l'$ with $l-l'$. It is invariant under the transformation $l \to 2\pi - l$ and $l' \to 2\pi - l'$. Since the measure also has the same invariance, it is a symmetry of the partition function. This is precisely the global center symmetry present in the Lagrangian formulation. Hence, the partition function in the strong coupling limit resembles that of a spin system with a global $Z(2)$ symmetry with a rather complicated looking interaction between the spins.

At low temperatures, the spins are disordered with

$$\langle \cos\Big(\frac{l(\vec{n})}{2}\Big)\rangle = 0 \tag{2.88}$$

and this corresponds to the phase of confined quarks in which the Wilson-Polyakov line has a zero expectation value. The correlation function falls exponentially at large distances as

$$\langle \cos\Big(\frac{l(\vec{n})}{2}\Big) \cos\Big(\frac{l(\vec{n}')}{2}\Big)\rangle = \exp(-\mu|\vec{n} - \vec{n}'|), \tag{2.89}$$

giving a linear confining potential between quarks.

At high temperatures, the spins of the model get aligned giving

$$\langle \cos\Big(\frac{l(\vec{n})}{2}\Big)\rangle \neq 0. \tag{2.90}$$

This state clearly breaks the global center invariance present in the partition function and corresponds to the phase of deconfined quarks in which the Wilson-Polyakov line has a non zero expectation value. The correlation function declines gradually as

$$\langle \cos\Big(\frac{l(\vec{n})}{2}\Big)\cos\Big(\frac{l(\vec{n}')}{2}\Big)\rangle = M^2(1 + c\exp(-\mu|\vec{n} - \vec{n}'|)), \tag{2.91}$$

giving a screened potential between quarks.

Since the above calculation was done in the strong coupling limit, it is natural to ask if the result will be valid for weak coupling ($g \to 0$), which is the region of physical interest. There are some rigorous proofs for the existence of a high temperature deconfining phase [10], which indicate that the result will also hold in the weak coupling limit. In the next section, we describe the Monte-Carlo method which enables us to handle the weak coupling region.

2.4 The Monte-Carlo Method

Lattice gauge theories in general are not amenable to exact analysis. However, their resemblance to statistical mechanical systems allows the application of several well known techniques like series and character expansions, duality transformations etc in their study. Despite the success of these methods in elucidating their properties, they are of limited applicability. Numerical Monte Carlo methods [6] on the other hand, are sufficiently general and can be employed with great effectiveness in addressing

a variety of issues. Their remarkable success in statistical and condensed matter physics makes them a promising tool in the study of lattice gauge theories. Since we have employed this method extensively in this thesis, we explain it here in some detail.

Expectation values in lattice gauge theories are given by

$$\langle O \rangle = \frac{\int [dU(n;\mu)] O[U] \exp(-\beta S(U))}{\int [dU(n;\mu] \exp(-\beta S(U))}, \tag{2.92}$$

where $O[U]$ is some observable expressed in terms of the link variables $U(n;\mu)$. The Monte-Carlo method evaluates this quantity by taking a statistical average of O over a large number of ensembles which are distributed according to the Boltzmann factor $\exp(-\beta S(U))$ present in the above integral. These ensembles are generated by using a dynamical probabilistic algorithm, by a process of continuous iteration.

Let $K_1, K_2 ... K_N$ be a sequence of ensembles of the link variables, which are distributed according to the Boltzmann law. The expectation value of O is approximated by

$$\langle O \rangle_{appr} = \frac{1}{N} \sum_{i=1,N} O(i), \tag{2.93}$$

where $O(i)$ is the value of the operator O in the ith ensemble. The error in this measurement is of the order of $\sqrt{\frac{\langle O^2 \rangle - \langle O \rangle^2}{N-1}}$, where N is the number of ensembles generated. The algorithm which generates these ensembles, is designed to produce an equilibrium distribution corresponding to a temperature β. Two commonly used ones are the heat bath and the Metropolis algorithms. They operate by starting from some arbitrary configuration and generating a sequence of configurations which ultimately converges to the Boltzmann distribution. We briefly explain these two algorithms. In this thesis we have used only the Metropolis method to make our simulations since it is easier to implement than the heat bath.

1.Heat Bath

In this method, a link variable $U(n;\mu)$ in a particular configuration is replaced by $U'(n;\mu)$ which is chosen with a probability density proportional to the Boltzmann factor

$$dP(U) = \exp(-\beta S(U))dU, \tag{2.94}$$

where $S(U)$ is the action of the background links which interact with this link. The process is repeated for all the links in a particular configuration. Clearly, this algorithm will lead to a thermal equilibrium.

2.Metropolis

In this method, a link variable $U(n;\mu)$ is replaced by new variable chosen at random and the change in the action (ΔS) is computed. If the action is lowered, the change is accepted unconditionally, otherwise, it is accepted with a probability $\exp(-\Delta S)$. This is accomplished by generating a random number x between zero and one, and the change is accepted if $\exp(-\Delta S) > x$. It is evident that after a large number of iterations, the Metropolis method will reduce to the heat bath method.

2.5 Monte-Carlo Results

In this section we briefly present some Monte-Carlo results which will be useful to us in our ensuing studies. Monte-Carlo simulations of the $SU(2)$ [8] and $SU(3)$ [18] LGTs indicate a phase transition to a high temperature deconfining phase. The Wilson line in the fundamental representation is an order parameter for this transition and becomes non zero at high temperatures while it remains zero at low temperatures. The global center symmetry is spontaneously broken in the high temperature phase. The nature of this transition is also well known. In the $SU(2)$

theory, the transition is of second order and has the same critical behaviour as the three dimensional Ising model [23]. The $SU(3)$ theory on the other hand, has a first order phase transition as in three dimensional $Z(3)$ spin models [18]. These observations are in conformity with the arguments presented by Svetitsky and Yaffe [9], who pointed out several common features between finite temperature phase transitions in gauge theories and those in spin models. There is also evidence [25] that suggests that these transitions will survive in the continuum limit, though scaling relations like Eq. 2.54 have not been completely established. The evidence from the behaviour of the Wilson lines, points to a high temperature deconfining phase. On the other hand, the area law behaviour of spatial Wilson loops [12], and the deviations [26] from ideal gas like behaviour at high temperatures, indicates the presence of non perturbative effects.

Monte-Carlo simulations of mixed action LGTs have also been performed. These LGTs have the same continuum limit as those defined using the fundamental Wilson action. However, LGTs defined with the fundamental Wilson action have a rich phase structure even at zero temperature. Recently, Gavai et al [13] studied the high temperature properties of an $SU(2)$ LGT, whose action [16] is the sum of the trace of the plaquette variables in the fundamental and adjoint representations. The action they studied is defined by

$$S = \frac{\beta_f}{2} \sum_{n\mu\nu} Tr_f U(n;\mu\nu) + \frac{\beta_a}{3} \sum_{n\mu\nu} Tr_a U(n;\mu\nu). \tag{2.95}$$

They found that the $SU(2)$ deconfinement transition (for $\beta_a = 0$), which is of second order, apparently joined the bulk phase transition in this model, which is of first order. Their observations are displayed in Fig 2.1. A similar merging of bulk and finite temperature transitions is seen in the phase diagram of the mixed action LGT

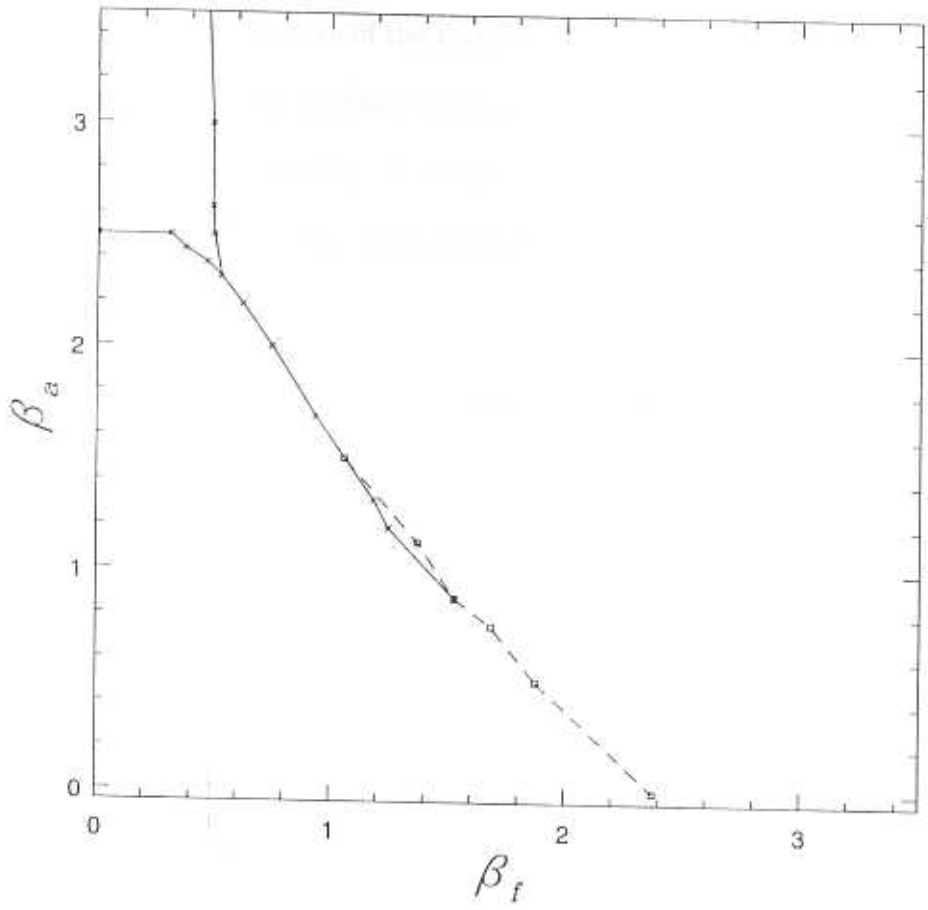

Fig. 2.1 The phase diagram of the Bhanot-Creutz model at zero and finite temperature.The bulk transition is shown by an unbroken line, while the dashed line is the finite temperature transition seen by Gavai et al.

for the group $SU(3)$ [14]. Various interpretations [13] have been proposed to explain these features. Taking the merging of the two transitions to be exact, the authors [13] have considered the possibility of there being only bulk or finite temperature transitions in the mixed action LGT. If the transitions are all bulk transitions, then it would mean the absence of any finite temperature transition in this model. On the other hand, if the transitions are all finite temperature transitions, this would mean that the transitions seen on symmetric lattices are all small volume effects of finite temperature transitions. Both these scenarios are difficult to reconcile with theoretical arguments and simulation results. The strong coupling approximation

and Monte-Carlo results for the pure gauge theory both indicate a finite temperature transition. The first order nature of the transitions seen on symmetric lattices makes it difficult to consider them as finite temperature transitions since this would go against the notion of universality. A milder possibility is that the merging of the transitions is not exact [13, 14]. This would mean that there are two transitions with different properties.

In the next chapters, we make a systematic study of the $SO(3)$ LGT and try to clarify these issues.

Chapter 3

Properties of the Wilson Line Variable

In this chapter we consider some properties of the Wilson line variable $L_f(\vec{x})$, which are useful in understanding its behaviour. It is defined as

$$L_f(\vec{x}) = Tr\ P\ \exp\Big(ig\int_0^\beta dx_4 A_4^a(\vec{x}, x_4)\tau^a/2\Big), \tag{3.1}$$

where the subscript f indicates that the trace is taken in the fundamental representation of $SU(2)$. The τ^as are the Pauli matrices. We will then consider the Wilson line variable defined in the adjoint representation.

In the Hamiltonian formulation, the partition function is

$$Z = Tr' \exp(-\beta H), \tag{3.2}$$

where the prime on the trace denotes that it is taken over the physical (gauge invariant) states. These states satisfy the Gauss law constraint, which can formally be written as

$$D_i E_i^a(\vec{x}) = 0 \tag{3.3}$$

in the absence of matter fields. In the strong coupling calculation of Z for the $SU(2)$ LGT[7], this constraint is implemented by using a Lagrange multiplier.

The partition function for the continuum theory in the imaginary time formulation is

$$Z = \int_{pbc} DA_\mu \exp\Big(-\frac{1}{2}\int_0^\beta dx_4 \int d^3x\ Tr(\partial_\mu A_\nu - \partial_\nu A_\mu + [A_\mu, A_\nu])^2\Big), \tag{3.4}$$

where $\mu = 1, 2, 3, 4$ and x_4 is the imaginary time. The suffix *pbc* indicates that the field configurations are periodic in x_4 with period β. Linearizing the quadratic term in $A_4^a(x)$ and introducing the auxiliary field $E_i^a(x)$, the partition function becomes

$$Z = \int_{pbc} DA_4^a DE_i^a DA_i^a \exp\Big(\int_0^\beta dx_4 \int d^3x \Big[iE_i^a(x)(D_i A_4^a(x) - \partial_4 A_i^a(x)) - (\frac{1}{2} E_i^a(x) E_i^a(x) + \frac{1}{2} B_i^a(x) B_i^a(x)) \Big] \Big). \quad (3.5)$$

Integrating over $A_4^a(x)$, gives the Gauss law constraint in Eq. 3.3. Using the Feynman time slicing procedure, $E_i^a(x)$ and $A_i^a(x)$ are recognized to be canonically conjugate, and the partition function can be written as

$$Z = Tr\ \exp(-\beta H) \prod_{\vec{x}a} \delta(D_i E_i^a(\vec{x})), \quad (3.6)$$

where

$$H = \frac{1}{2} \int d^3x (E_i^a(\vec{x}) E_i^a(\vec{x}) + B_i^a(\vec{x}) B_i^a(\vec{x})). \quad (3.7)$$

This clarifies the connection with the Hamiltonian formalism.

3.1 The Wilson line in the fundamental representation.

We now consider the meaning of the correlations

$$\langle L_f(\vec{x}_1) L_f(\vec{x}_2) .. L_f(\vec{x}_n) \rangle \quad (3.8)$$

of the Wilson line variable defined in the fundamental representation. Using a fermionic representation [32], $L_f(\vec{x})$ can be expressed as the path integral

$$L_f(\vec{x}) = \int d\eta(\vec{x}, x_4) d\bar{\eta}(\vec{x}, x_4) \bar{\eta}(\vec{x}, \beta) \eta(\vec{x}, 0) \exp\Big(\int dx_4 \bar{\eta}(\vec{x}, x_4)(\partial_4 - igA_4^a(\vec{x}, x_4)\tau^a/2) \eta(\vec{x}, x_4) \Big), \quad (3.9)$$

where the $\eta(x)$s are Grassmann variables defined in the fundamental representation of $SU(2)$. In this representation, the Wilson line is the amplitude for the Grassmann variables $(\eta(\vec{x},\tau),\bar{\eta}(\vec{x},\tau))$ coupled minimally to the gauge field and moving along the world line $(\vec{x},\tau)$. The Grassmann variables satisfy antiperiodic boundary conditions

$$\eta(\vec{x},\beta) = -\eta(\vec{x},0),$$
$$\bar{\eta}(\vec{x},\beta) = -\bar{\eta}(\vec{x},0).$$

Substituting in Eq. 3.5, and integrating over $A_4^a(x)$ one obtains the constraints

$$D_i E_i^a(\vec{x}) = g\bar{\eta}(\vec{x})(\tau^a/2)\eta(\vec{x}). \tag{3.10}$$

The Gauss law is modified at the spatial location of the Wilson line, by a fermionic source in the appropriate representation. Therefore we have

$$\langle L_f(\vec{x}_1)L_f(\vec{x}_2)..L_f(\vec{x}_n)\rangle = \exp\Big(-\beta[F(\vec{x}_1,\vec{x}_2,..\vec{x}_n) - F(0)]\Big)$$

where $F(\vec{x}_1,\vec{x}_2..\vec{x}_n)$ is the free energy of static sources located at $\vec{x}_1,\vec{x}_2..\vec{x}_n$ and $F(0)$ is the free energy in the absence of any static sources.

In[28] it is claimed that $\langle L_f(\vec{x})L_f(\vec{0})\rangle$ correlations are related to the free energies of the static quark-antiquark pair in both the colour singlet and colour triplet configurations. Our derivation above shows that only the colour singlet configuration contributes.

Note that we have the freedom of using just one Lagrange multiplier (for each $\vec{x}$) in Eq. 3.6 and Eq. 3.2, instead of one at each x_4 of the Feynman time slicing, as provided by $A_4(\vec{x},x_4)$. These two choices are equivalent, since the Gauss law constraint commutes with the Hamiltonian, and its imposition at one x_4 requires it to be preserved for all x_4. In the Lagrangian formalism this is reflected (see Eq. 3.5)

as follows. By a local gauge transformation one may almost, but not quite, make $A_4^a(\vec{x}, x_4) = 0$. If $u(\vec{x}) \neq 1$, where

$$u(\vec{x}) = P \exp\Big(ig \int_0^\beta dx_4 A_4^a(\vec{x}, x_4)\tau^a/2\Big), \tag{3.11}$$

then $A_4^a(\vec{x}, x_4)$ can be gauge transformed to zero everywhere except in an arbitrarily short interval. Equivalently, $A_4^a(\vec{x}, x_4)$ can be made to be a constant $A_4^a(\vec{x})$, which is independent of x_4 such that

$$u(\vec{x}) = \exp\Big(ig\beta A_4^a(\vec{x})\tau^a/2\Big). \tag{3.12}$$

All this amounts to saying that the entire gauge invariant content of $A_4^a(\vec{x}, x_4)$ is contained in the group element $u(\vec{x})$. We can write

$$u(\vec{x}) = \exp\Big(i\phi^a(\vec{x})\tau^a/2\Big), \tag{3.13}$$

where $\vec{\phi}$ parametrizes the elements of the group $SU(2)$. It is this variable which enters as the Lagrange multiplier field in the analysis of the strong coupling limit of the $SU(2)$ LGT [7]. To impose the δ-function constraint in Eq. 3.6, we have to integrate over $\vec{\phi}$ using the $SU(2)$ Haar measure $4(\sin^2|\vec{\phi}|/2)d|\vec{\phi}|d^2\hat{\phi}$.

Let us imagine integrating over the $A_i^a(x)$ and $E_i^a(x)$ variables, to express Z in terms of $A_4^a(x)$ only (as is done in the strong coupling limit). $u(\vec{x})$ transforms homogeneously under local gauge transformations as

$$u(\vec{x}) \to V(\vec{x}, 0)u(\vec{x})V^\dagger(\vec{x}, 0) \tag{3.14}$$

because of the periodicity in the x_4 direction. Therefore, only the eigenvalues of $u(\vec{x})$ enter in the expression for the partition function, Z. In case of $SU(2)$, this means that Z is expressible in terms of $|\vec{\phi}(\vec{x})|$ only. Z has the global $Z(2)$ invariance

$$|\vec{\phi}| \to 2\pi - |\vec{\phi}| \tag{3.15}$$

for all $\vec{x}$. The high temperature phase is characterized by a spontaneous breaking of this global symmetry. Thus $|\vec{\phi}|$ is a disorder parameter for this transition.

Naively, it would appear that one could simply consider the expectation value $\langle L_f(\vec{x})\rangle$ in the fundamental representation. This would directly give $\exp(-\beta\Delta F)$ where ΔF is the free energy of a static quark immersed in the heat bath of gluons. If $\langle L_f(\vec{x})\rangle$ is zero for $T \leq T_c$, an isolated quark has infinite free energy, implying confinement. It has been noted in literature [24] that the free energy interpretation for $\langle L_f(\vec{x})\rangle$ requires $\exp(-\beta\Delta F)$ and therefore $\langle L_f(\vec{x})\rangle$ to be positive definite. But the high temperature phase has two equivalent ground states, in one of which $\langle L_f(\vec{x})\rangle$ is negative. Thus one has a contradiction.

This contradiction can be resolved by noting that $\langle L_f(\vec{x})\rangle$ is identically zero at any temperature. There are simply no states satisfying the Gauss law constraint to the trace in Eq. 3.6. The Gauss law requires a string of half integer electric flux to start from $\vec{x}$. There is no way of satisfying the source free Gauss law at the other end of the string.

On the other hand, $\langle L_f(\vec{x})L_f(\vec{0})\rangle$ does not suffer from this problem. Now the string starting at $\vec{x}$ can end at $\vec{0}$ and so there are physical states contributing to the trace in Eq. 3.6. This quantity is positive definite and there is no contradiction with the free energy interpretation.

This situation can be contrasted with that of a conventional spin system, for e.g. the Ising model. There, the expectation value $\langle S(\vec{x})\rangle$ of a single spin is identically zero in any finite volume. The reason is however different. In a finite volume there can be no spontaneous symmetry breaking, since there is always tunnelling between configurations with opposite signs of $S(\vec{x})$ to give $\langle S(\vec{x})\rangle = 0$. Only in an infinite

volume system (or at $T = 0$), can we get $\langle S(\vec{x}) \rangle \neq 0$ with all the spins aligned in a single direction. In contrast, even in an infinite volume, $\langle L_f(\vec{x}) \rangle = 0$ simply because there are no states satisfying the Gauss law. We can arrange the other end of the string to be at infinity, but this amounts to introducing a static anti-quark at infinity.

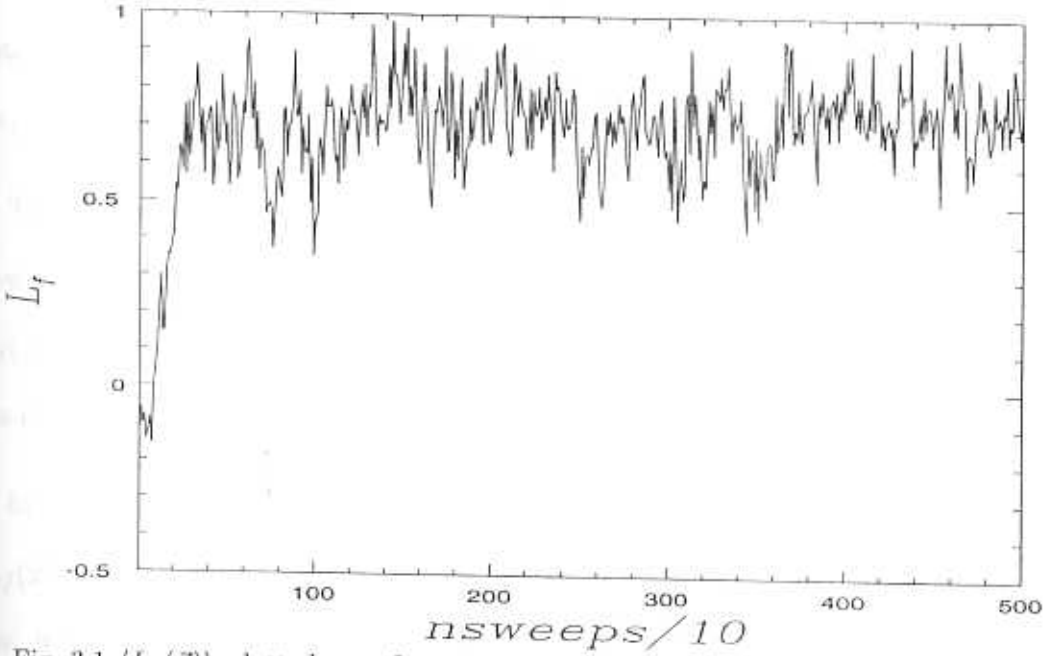

Fig. 3.1 $\langle L_f(\vec{x}) \rangle$ plotted as a function of number of sweeps for the $SU(2)$ theory at high temperatures.

Apart from the above difference, the signal for spontaneous symmetry breaking is the same in both systems. If $\lim_{|\vec{x}| \to \infty} \langle L_f(\vec{x}) L_f(\vec{0}) \rangle = |\langle L_f(\vec{0}) \rangle|^2 \neq 0$, then the $Z(2)$ symmetry is spontaneously broken. Though this variable directly does not show that there are two degenerate ground states, the $Z(2)$ symmetry assures us that if there is a ground state with $\langle L_f(\vec{x}) \rangle$ configurations predominantly having a common sign everywhere, then there is another ground state with $\langle L_f(\vec{x}) \rangle$ having predominantly the opposite sign.

It is not difficult to see the degenerate ground states in simulations. Even though

there is no phase transition possible in the finite systems used in simulations, there is always tunnelling between possibly degenerate states in a finite volume V, with probability $\exp(-\alpha V)$, where α is a positive constant. This lifts the degeneracy between the ground states, and the symmetry gets restored. However, even in systems of small size, this probability is so small that the system remains trapped in a single ground state long enough for it to be considered as an equilibrium ground state in the simulations. In the Ising model, the average value of a spin at a given site, will settle into one of equal but opposite non zero values.

The situation is no different for $\langle L_f(\vec{x})\rangle$ in the $SU(2)$ LGT. Even though we have argued that $\langle L_f(\vec{x})\rangle$ is strictly zero due to the Gauss law, the average value of $\langle L_f(\vec{x})\rangle$ behaves like $S(\vec{x})$ in the Ising model at high temperatures. Fig 3.1 illustrates this behaviour.

In recent simulations, $\langle |L_f(\vec{x})|\rangle$ is almost always used to probe the system, but $\langle |L_f(\vec{x})|\rangle$ is never zero, and hence not an order parameter in the strict sense. However, it is more instructive and not more difficult to use $\langle L_f(\vec{x})\rangle$ (averaged over a certain number of sweeps). In addition to being a true order parameter, it provides more information about the system.

3.2 The Wilson line in the adjoint representation.

We will now consider $L_a(\vec{x})$, i.e the Wilson line variable in the adjoint representation of $SU(2)$. This plays a crucial role in this thesis. It is defined as

$$L_a(\vec{x}) = Tr\ P\ \exp\Big(ig\int_0^\beta dx_4 A_4^a(\vec{x},x_4)T^a\Big), \tag{3.16}$$

where the subscript a indicates that the trace is taken in the adjoint representation of $SU(2)$. The T^as are matrices in the adjoint representation of $SU(2)$.

We should not expect $\langle L_a(\vec{x})\rangle$ to be identically zero because of the inability of states to satisy the Gauss law. A static quark in the adjoint representation of $SU(2)$ can form a colour singlet bound state with a gluon, and therefore satisfy the Gauss

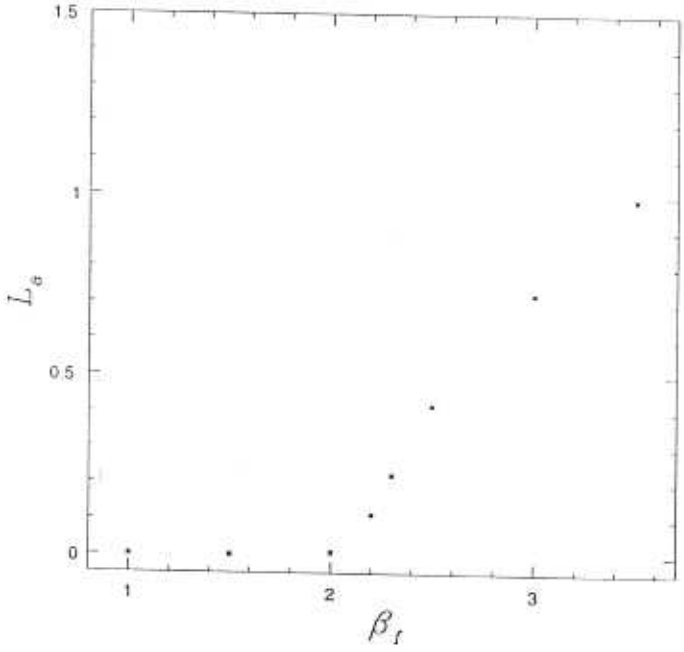

Fig. 3.2 $\langle L_a\rangle$ for the $SU(2)$ theory on a 7^3 3 lattice.

law. In the Hamiltonian formulation of LGT, this corresponds to a loop of electric flux (of either 1/2 or 1 unit) starting and ending at the static quark. At $T = 0$ in the strong coupling expansion, the leading contribution is due to a loop spanning one plaquette, and the energy is $\Delta E = k\beta_f^4 + O(\beta_f^6)$. This gives a contribution $\exp(-k\beta\beta_f^4)$ to $\langle L_a(\vec{x})\rangle$. We remark here that for the lattices and couplings used in numerical simulations, this is very small.

The observable $\langle L_a(\vec{x})\rangle$ is invariant under the $Z(2)$ transformation because the adjoint representation of $SU(2)$ has center charge zero. This means that $\langle L_a(\vec{x})\rangle$ will

have the same value for the two degenerate ground states of the high temperature phase of the $SU(2)$ theory. Thus, probing the system using $\langle L_a(\vec{x})\rangle$, we can detect the finite temperature transition by a jump in $\langle L_a(\vec{x})\rangle$. But, neither is $\langle L_a(\vec{x})\rangle$ strictly zero in the low temperature phase, nor do we see a double valuedness in its value in the high temperature phase. Nonetheless, $\langle L_a(\vec{x})\rangle$ is so small in the low temperature phase, that it is zero within errors in the simulation (Fig. 3.2). Also, $\langle L_a(\vec{x})\rangle$ becomes non-zero at the same value as $\langle L_f(\vec{x})\rangle$ ($\beta_f = 2.2$ on a 7^3 3 lattice). (In Fig. 3.2 we have plotted the value of $L_a(\vec{n})$ averaged over all lattice sites, which we have denoted by L_a.) Hence it seems to be an equally good observable to locate the finite temperature transition in the $SU(2)$ LGT. In the next chapter, we shall use $\langle L_a(\vec{x})\rangle$ to study the high temperature phase of the $SO(3)$ LGT.

The properties of $\langle L_a(\vec{x})\rangle$ in the high temperature phase of the $SU(2)$ LGT have been studied [29]. It is also noted there that in the $SU(2)$ LGT, the adjoint Wilson line becomes non zero at the same temperature as the fundamental Wilson line. The Wilson line defined in higher representations [30] has also been studied recently. Similar studies have also been performed for the group $SU(3)$ [31].

Chapter 4

Study of the SO(3) lattice gauge theory.

In this chapter, we study the finite temperature properties of the adjoint $SU(2)$ LGT, whose action is defined by

$$S = \frac{\beta_a}{3} \sum_{n\mu\nu} Tr_a U(n;\mu\nu). \tag{4.1}$$

The subscript a denotes the trace in the adjoint representation of $SU(2)$. The trace of an $SU(2)$ group element in the adjoint representation is related to that in the fundamental representation by

$$Tr_a U = (Tr_f U)^2 - 1 \quad . \tag{4.2}$$

Unlike the fundamental Wilson action

$$S = \frac{\beta_f}{2} \sum_{n\mu\nu} Tr_f U(n;\mu\nu), \tag{4.3}$$

which defines the $SU(2)$ LGT, the adjoint action describes the $SO(3)$ LGT, since the $SU(2)$ link variables $U(n;\mu)$ and $-U(n;\mu)$ have the same weight. Even though the link variables are $SU(2)$ matrices and the measure in the path integral is the $SU(2)$ Haar measure, the adjoint action is equivalent to the $SO(3)$ LGT which uses $SO(3)$ matrices as its fundamental variables. It has the same classical continuum limit as the Wilson action. In this limit, the couplings of the two theories are related by (see Eq. 2.59)

$$\beta_f = \frac{8}{3}\beta_a. \tag{4.4}$$

The zero temperature properties of the $SO(3)$ LGT are well known [17, 19]. It has a first order transition at $\beta_a \approx 2.6$, which is driven by a condensation of $Z(2)$ monopoles[19]. The $Z(2)$ monopoles are configurations which carry a $Z(2)$ magnetic flux inside a three dimensional cube. The $Z(2)$ monopole density in a 3 dimensional cube is defined as

$$\rho(c) = \frac{1}{2}(1 - sgn(\prod_{p \in \partial c} U(p))). \tag{4.5}$$

This transition is a confinement to confinement transition. Since it occurs at a finite value of β_a, it is irrelevant for the continuum limit (which is at $\beta_a = \infty$).

We are interested in the finite temperature properties of the $SO(3)$ LGT for many reasons. Firstly, the group $SO(3)$ has a trivial center subgroup. The center of $SU(2)$ ($Z(2)$) plays an important role in the deconfinement transition in the $SU(2)$ LGT[9]. Since the $SU(2)$ and $SO(3)$ theories are expected to have the same continuum limit, it would be interesting to see how the $SO(3)$ theory reproduces the same features as the $SU(2)$ theory. Secondly, the $SO(3)$ theory has a phase transition at zero temperature, which is well understood [19] to be a result of $Z(2)$ monopole condensation, and may perhaps be useful in explaining its finite temperature properties. We would also like to clarify the situation regarding the mixing of the bulk and finite temperature transitions, which is seen in mixed action LGTs [13, 14]. As we will see, $SO(3)$ LGT is the simplest model exhibiting the mixing of bulk and finite temperature effects.

The finite temperature properties of this model are calculated from the partition function

$$Z = \int dU(n;\mu) \exp\Big(\frac{\beta_a}{3} \sum_{n\mu\nu} Tr_a U(n;\mu\nu)\Big). \tag{4.6}$$

We first note that the global $Z(2)$ symmetry present in the Wilson action is now

promoted to a local symmetry in the adjoint action. This is because the transformation

$$U(\vec{n};\hat{4}) \rightarrow Z(\vec{n})U(\vec{n};\hat{4}) \tag{4.7}$$

is a symmetry of the action, where $Z(\vec{n}) = \pm 1$ and can now depend on the spatial position $\vec{n}$. In the Hamiltonian formalism, the strong coupling limit yields a spin model with a local $Z(2)$ invariance (see Appendix B). Under the local $Z(2)$ transformation, the Wilson line transforms as

$$L_f(\vec{n}) \rightarrow Z(\vec{n})L_f(\vec{n}). \tag{4.8}$$

Elitzur's theorem [22] dictates that such local symmetries can never be broken and therefore

$$\langle L_f(\vec{n})\rangle = 0. \tag{4.9}$$

The Wilson line expectation value is always zero, and hence it cannot be used as an order parameter to study the finite temperature transition in this model. Even the correlation function between two Wilson lines

$$\langle L_f(\vec{n})L_f(\vec{n}')\rangle = 0 \tag{4.10}$$

at all temperatures, because a non zero value will break the local $Z(2)$ symmetry.

For any observable to have a non zero expectation value, it must be invariant under the local center transformation in Eq. 4.7. A possible candidate is $L_a(\vec{n})$, the Wilson line in the adjoint representation. It is defined as

$$L_a(\vec{x}) = Tr\ P\ \exp\Big(ig\int_0^\beta dx_4 A_4^\alpha(\vec{x},x_4)T^\alpha\Big), \tag{4.11}$$

where T^αs are the matrices in the adjoint representation of $SU(2)$. It has the physical interpretation of measuring the free energy $(F_a(\vec{n}))$ of a static adjoint quark when

written as

$$\langle L_a(\vec{n})\rangle = \exp\Big(-\beta[F_a(\vec{n}) - F(0)]\Big). \tag{4.12}$$

For the group $SU(2)$, $L_a(\vec{n})$ and $L_f(\vec{n})$ are related by

$$L_a(\vec{n}) = L_f^2(\vec{n}) - 1. \tag{4.13}$$

The trace of the Wilson lines in the fundamental and adjoint representations can be written as $L_f(\vec{n}) = 2\cos(\frac{\theta(\vec{n})}{2})$ and $L_a(\vec{n}) = 1 + 2\cos(\theta(\vec{n}))$ respectively, where $\exp(\pm\frac{i\theta(\vec{n})}{2})$ are the eigenvalues of the Wilson line. The $\theta(\vec{n})$s are gauge invariant observables, and the center transformation on them is

$$\theta(\vec{n}) \to 2\pi - \theta(\vec{n}). \tag{4.14}$$

This changes the sign of $L_f(\vec{n})$ but leaves $L_a(\vec{n})$ unchanged. Hence $L_a(\vec{n})$ is an interesting observable, which can be studied to see if it displays any characteristic behaviour. However, there is no reason to expect $\langle L_a(\vec{n})\rangle$ to be zero even at low temperatures, since an adjoint quark can always form a colour singlet bound state with a gluon.

We now make a numerical study of the $SO(3)$ LGT (see Appendix A for more details of the simulation). We consider the behaviour of the adjoint Wilson line, the $Z(2)$ monopole density, and the energy density which is defined as $E = 1 - \frac{1}{3}Tr_a U(p)$ for every plaquette. We measure the spatial averages of these variables, which are defined as

$$L_a = \frac{1}{N_\sigma}\sum_{\vec{n}} L_a(\vec{n}), \tag{4.15}$$

$$P = \frac{1}{N_{pl}}\sum_{p}(1 - \frac{1}{3}Tr_a U(p)), \tag{4.16}$$

and

$$\rho = \frac{1}{N_c}\sum_{c}\rho(c) \quad . \tag{4.17}$$

In the above definitions, N_σ,N_{pl} and N_c are the number of sites, plaquettes and three dimensional cubes respectively. We have measured $\langle L_a \rangle$ on a 7^3 3 lattice and find

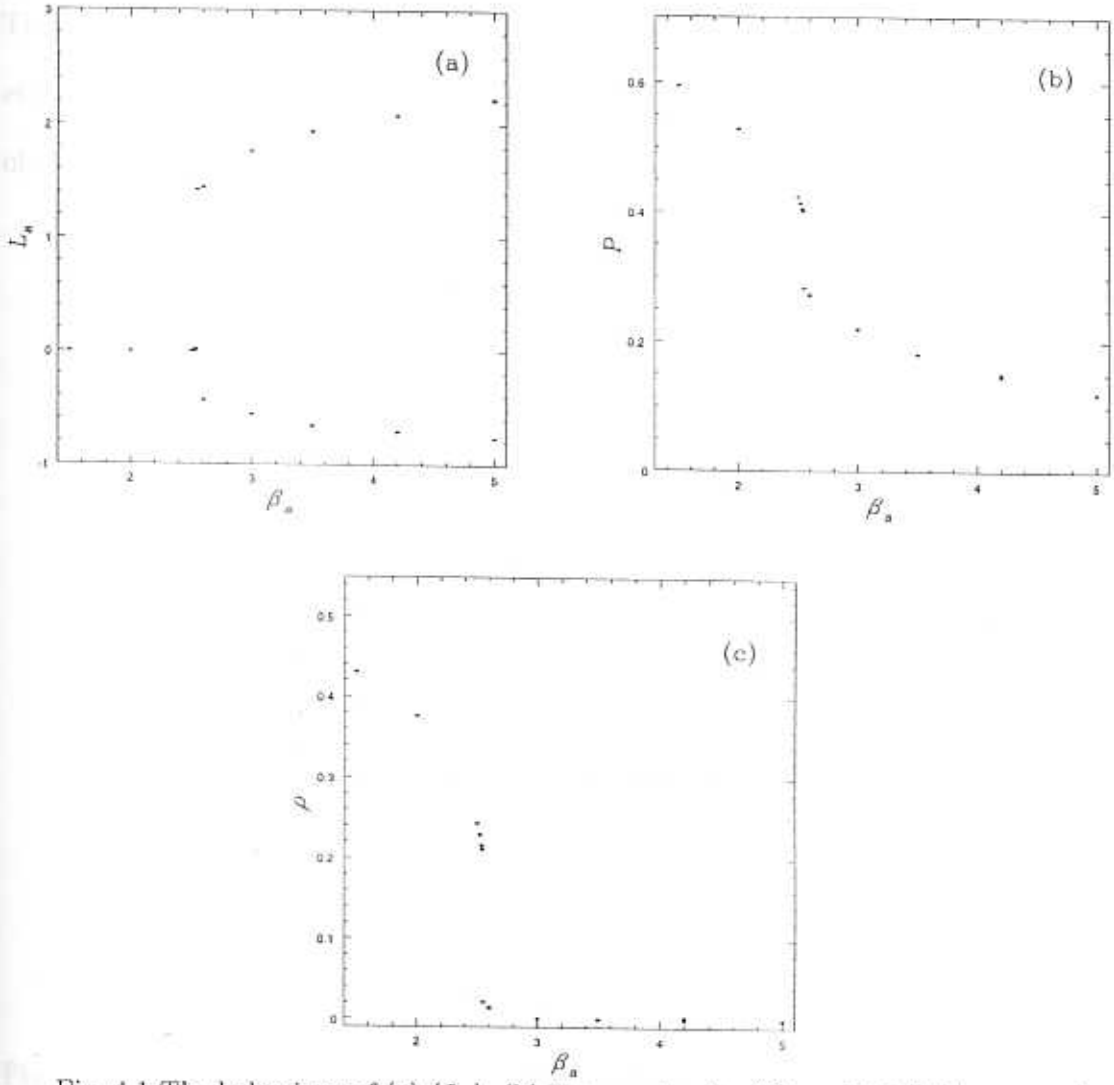

Fig. 4.1 The behaviour of (a) $\langle L_a \rangle$, (b) Energy density (P) and (c) $Z(2)$ monopole density(ρ) on a 7^3 3 lattice.

that it is very small (Fig. 4.1a) in the low temperature phase (small β_a), though there is no reason for it to be exactly zero. This behaviour can be understood from the strong coupling expansion. The strong coupling expansion gives

$$\langle L_a \rangle \approx (\beta_a/3)^{4N_\tau}, \tag{4.18}$$

which is very small for the couplings and lattices we are considering. This is presum-

ably the reason for the smallness of $\langle L_a \rangle$ at low temperatures. At high temperatures (β_a large), $\langle L_a \rangle \neq 0$ and it jumps abruptly across some critical value ($\beta_a \approx 2.6$). Thus it is an observable which can detect a transition, like any other order parameter. Fig 4.1a shows the variation of $\langle L_a \rangle$ with β_a on a 7^3 3 lattice. The variation of the energy density (P) and the $Z(2)$ monopole density (ρ) are also shown (see

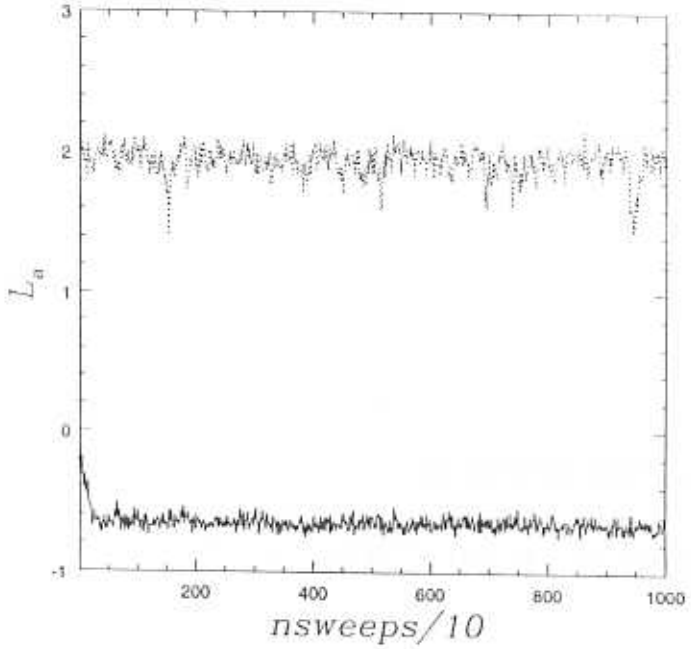

Fig. 4.2 L_a plotted against the number of Monte-Carlo sweeps on a 7^3 3 lattice with a hot start (unbroken lines) and a cold start (broken lines). The value of $\beta_a = 3.5$.

Fig. 4.1b and Fig. 4.1c). The rapid fall in the energy density at $\beta_a \approx 2.6$ indicates a first order transition. This transition is driven by a decondensation of $Z(2)$ monopoles since their density drops drastically for $\beta_a > 2.6$.

An unexpected feature is that $\langle L_a \rangle$ takes two possible values at high temperatures, one of which is positive, while the other is negative. The value of $\langle L_a \rangle$ attained in the high temperature phase seems to depend on the initial configuration in the Monte-Carlo simulation. We find that a random configuration (hot start) settles down to either a positive or negative value of $\langle L_a \rangle$, while an ordered configuration

(cold start) always prefers the $\langle L_a \rangle$ positive value (Fig 4.2). Since the system spends a very long time in each of these states (we have not seen any tunnelling events till 100000 sweeps), we can make meaningful measurements of various quantities. We have measured the energies of these two states, and find that they are very close to each other, though the state with $\langle L_a \rangle$ positive seems to have a marginally lower energy. Since there is no symmetry requiring the presence of degenerate ground states, we expect that their energies are different, if only by a small amount. In that case, the energy gap between the two states will increase as the thermodynamic limit is reached, and the state with $\langle L_a \rangle$ positive will be the equilibrium phase. We will return to the question of the energy difference between these two states later on in this chapter. The $Z(2)$ monopole density is very small at high temperatures in both these states. In the plots shown in Fig. 4.1, the points showing the values of the energy density and $Z(2)$ monopole density for the two states, almost coincide.

We would like to understand the nature of this transition and the structure of the high temperature phase. In order to make a closer study of the two high temperature states, we have obtained the single site histograms for $L_a(\vec{n})$ at low and high temperatures. The histogram for $L_a(\vec{n})$ at low temperatures (Fig. 4.3b) shows that the configurations are peaked around $L_a(\vec{n}) \approx -1$, though there are also significant contributions from configurations with positive $L_a(\vec{n})$. The net effect is a very small value of $\langle L_a \rangle$ (almost zero). At high temperatures, the histogram shows a peaking of configurations at positive values for the state with $\langle L_a \rangle$ positive (Fig. 4.4b) and at -1 for the state with $\langle L_a \rangle$ negative (Fig. 4.9b).

We will now show that the state with $\langle L_a \rangle$ positive is like the high temperature deconfining phase of the $SU(2)$ theory. We present similar histograms for the $SU(2)$ theory in the low and high temperature phases (Fig. 4.5 and Fig. 4.6). In the $SU(2)$

theory, $\langle L_f \rangle$ is non zero and degenerate at high temperatures. The two degenerate values of $\langle L_f \rangle$ are related by a global $Z(2)$ transformation. In the last chapter, we showed that $\langle L_a \rangle$ is also non zero at high temperatures and takes the same value for

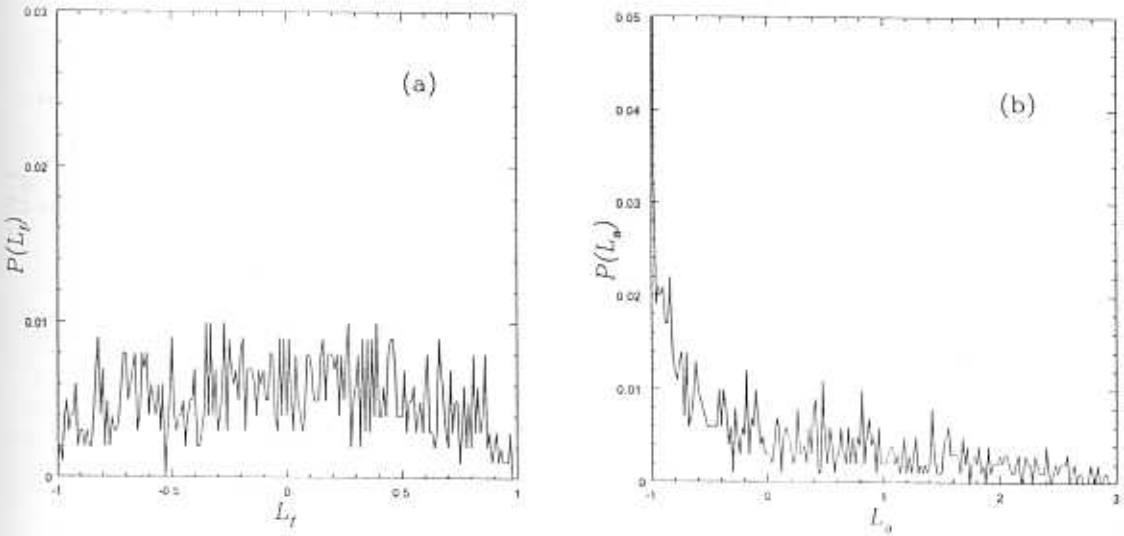

Fig. 4.3 Distribution of (a) $L_f(\vec{n})$ and (b) $L_a(\vec{n})$ in the low temperature phase of the $SO(3)$ theory. This is on a 7^3 3 lattice with $\beta_a = 2.0$.

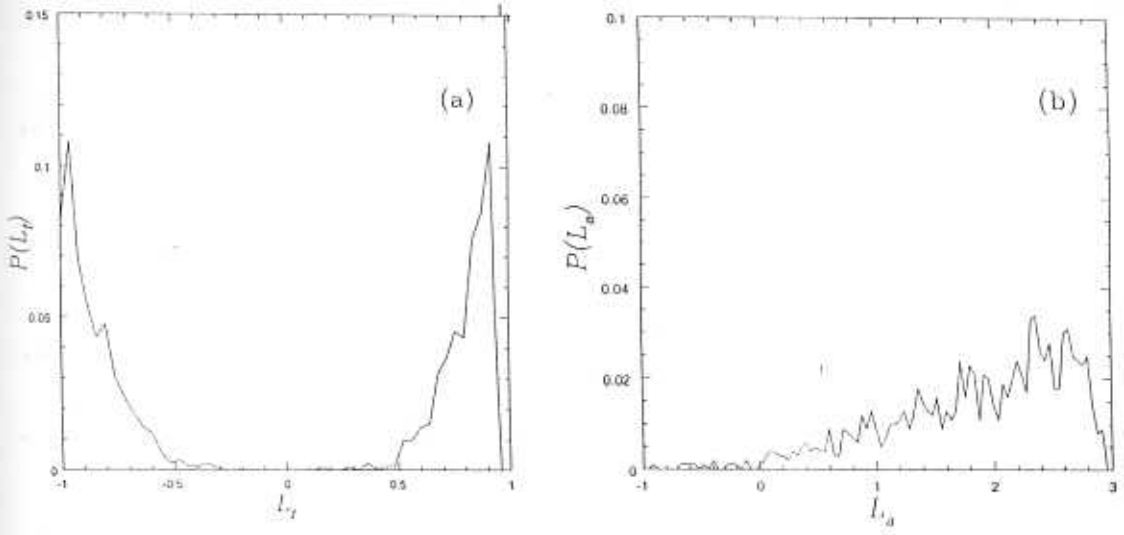

Fig. 4.4 Distribution of (a) $L_f(\vec{n})$ and (b) $L_a(\vec{n})$ in the $SO(3)$ theory at high temperatures for the $\langle L_a \rangle$ positive state. This is on a 7^3 3 lattice with $\beta_a = 3.5$.

either of the $Z(2)$ related values of $\langle L_f \rangle$. At low temperatures, both $\langle L_f \rangle$ and $\langle L_a \rangle$ are very small. Note the similarity in the histograms for $L_a(\vec{n})$ in the $\langle L_a \rangle$ positive

state of the $SO(3)$ theory and the high temperature phase of the $SU(2)$ theory. Both these histograms show a peaking of configurations in the positive region of $L_a(\vec{n})$. After comparing them, we can conclude that the state with $\langle L_a \rangle$ positive in the

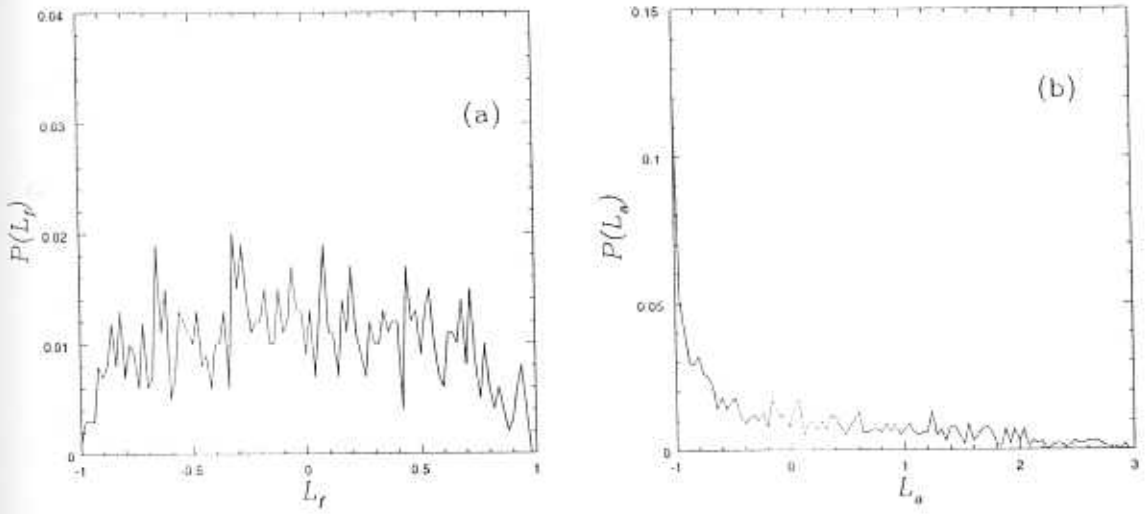

Fig. 4.5 Distribution of (a) $L_f(\vec{n})$ and (b) $L_a(\vec{n})$ in the low temperature phase of the $SU(2)$ theory. This is on a 7^3 3 lattice with $\beta_f = 1.5$.

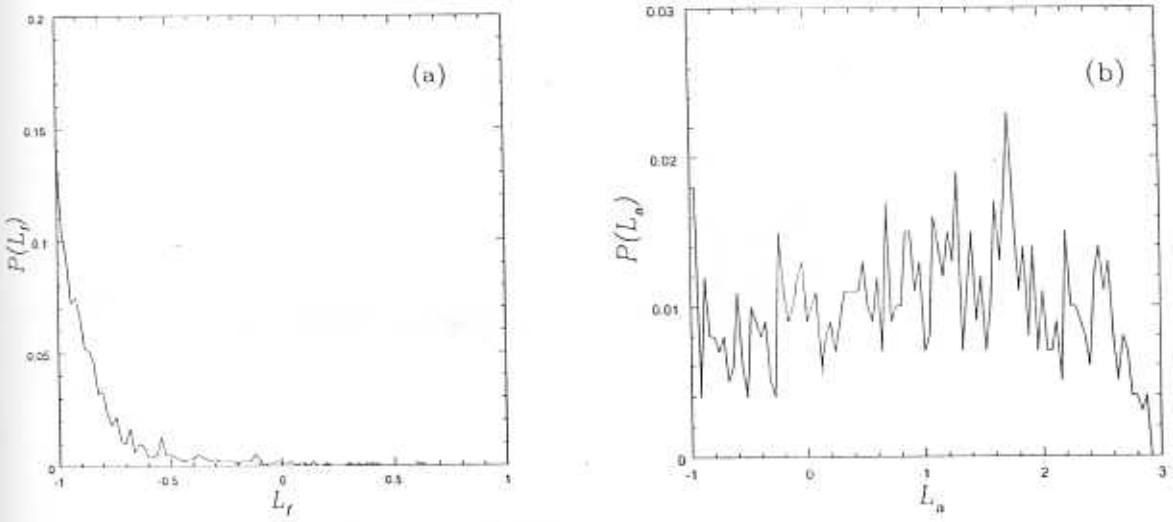

Fig. 4.6 Distribution of (a) $L_f(\vec{n})$ and (b) $L_a(\vec{n})$ in the high temperature phase of the $SU(2)$ theory. The value of $\beta_f = 3.5$.

$SO(3)$ theory is like the high temperature phase of the $SU(2)$ theory. A comparison of the numerical values of $\langle L_a \rangle$ in this state with those in the high temperature

phase of the $SU(2)$ LGT at related couplings (see Eq. 4.4), shows a good agreement which improves at larger values of β_f (β_a) (Fig 4.7b). Since the energy density is

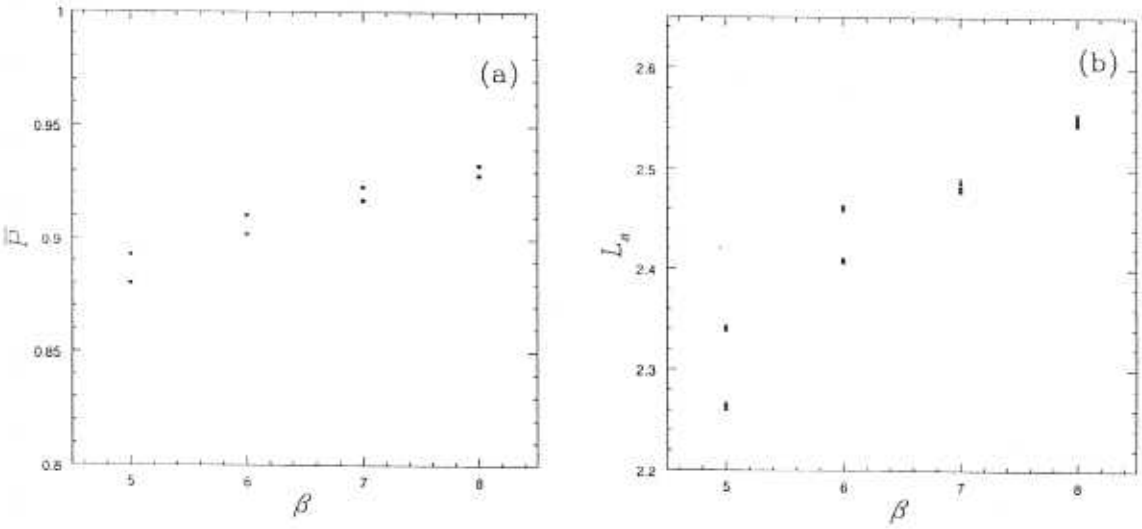

Fig. 4.7 Comparison of (a)$\bar{P}$ and (b)$\langle L_a \rangle$ for the $SU(2)$ (closed points) and $SO(3)$ (open points) theories at corresponding values of β_f and β_a.

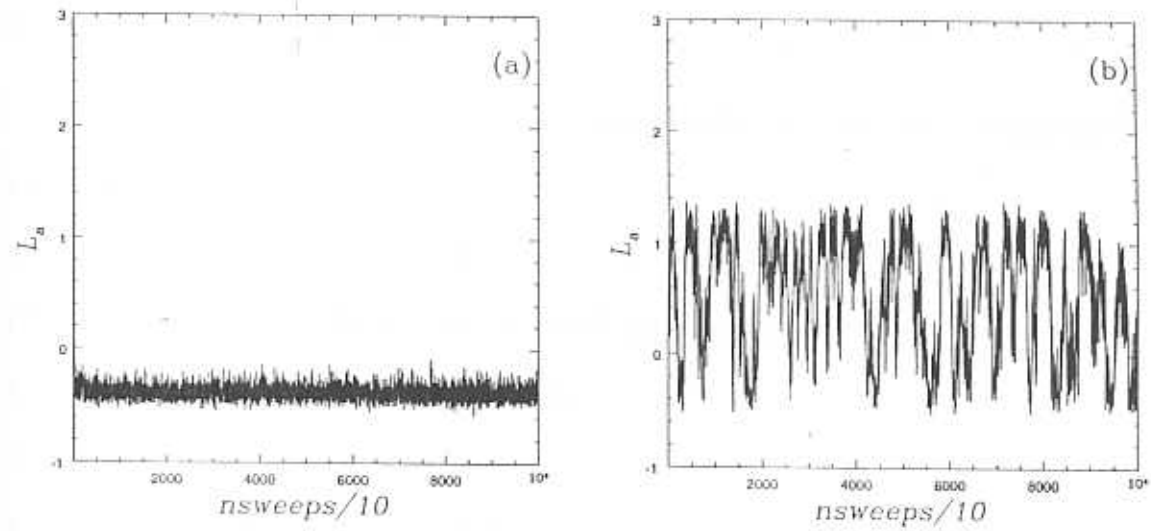

Fig. 4.8 Behaviour of L_a as a function of Monte-Carlo sweeps on a symmetric (7^4) lattice at $\beta_a = 3.5$ for (a) hot start and (b) cold start.

defined differently in the two theories ($P = 1 - \frac{1}{2}Tr_f U(p)$ in the $SU(2)$ theory and $P = 1 - \frac{1}{3}Tr_a U(p)$ in the $SO(3)$ theory), we cannot compare them directly. Instead, we can compare the values of an observable which is defined in the same way for

both theories, e.g. $\frac{1}{4}(Tr\ U(p))^2$. Its values (shown as $\bar{P}$ in Fig. 4.7a) in the high temperature phase of the $SU(2)$ theory and the $\langle L_a \rangle$ positive state of the $SO(3)$ theory (at couplings related as in Eq. 4.4) are shown to approach the same value. The $Z(2)$ monopole density is also very small (almost zero) in both cases. These observations provide further evidence that the high temperature phase of the $SU(2)$ theory and the $\langle L_a \rangle$ positive state of the $SO(3)$ theory are the same.

The corresponding $L_f(\vec{n})$ histograms are also shown. At low temperatures, they are peaked around zero in both the $SU(2)$ and $SO(3)$ theories (Fig. 4.5a and Fig. 4.3a). At high temperatures, the $L_f(\vec{n})$ histogram for the $SO(3)$ theory in the $\langle L_a \rangle$ positive state is a double peak distributed symmetrically about zero (Fig. 4.4a). This is expected from local $Z(2)$ invariance. The $L_f(\vec{n})$ histogram for the $SU(2)$ theory shows a peaking at positive or negative values, depending on the $Z(2)$ sector it gets trapped into (Fig. 4.6a).

The state with $\langle L_a \rangle$ negative is absent in the $SU(2)$ model, and we must seek elsewhere for an explanation. We will show that this is the bulk phase of the $SO(3)$ theory (at large β_a), at high temperatures. To see this, let us study the behaviour of $\langle L_a \rangle$ on a symmetric lattice, in the $SO(3)$ theory. In the thermodynamic limit, this would correspond to the zero temperature situation. At zero temperature, $\langle L_a \rangle$ is expected to be zero, but on finite lattices it will not be zero. We have measured $\langle L_a \rangle$ on a symmetric 7^4 lattice and find that it too has an unusual behaviour. Depending on the initial Monte-Carlo configuration, L_a settles down to a negative value (Fig. 4.8a) for a hot start or oscillates between negative and positive values without settling down to any particular value (Fig. 4.8b) for a cold start. This behaviour persists for a very large number (100000) of Monte-Carlo sweeps. Since the state reached by the hot start is the one more likely to be the true ground state,

we regard this as reasonable evidence for the $\langle L_a \rangle$ negative state to be the ground state. We have also obtained the single site histograms for $L_f(\vec{n})$ and $L_a(\vec{n})$ in this

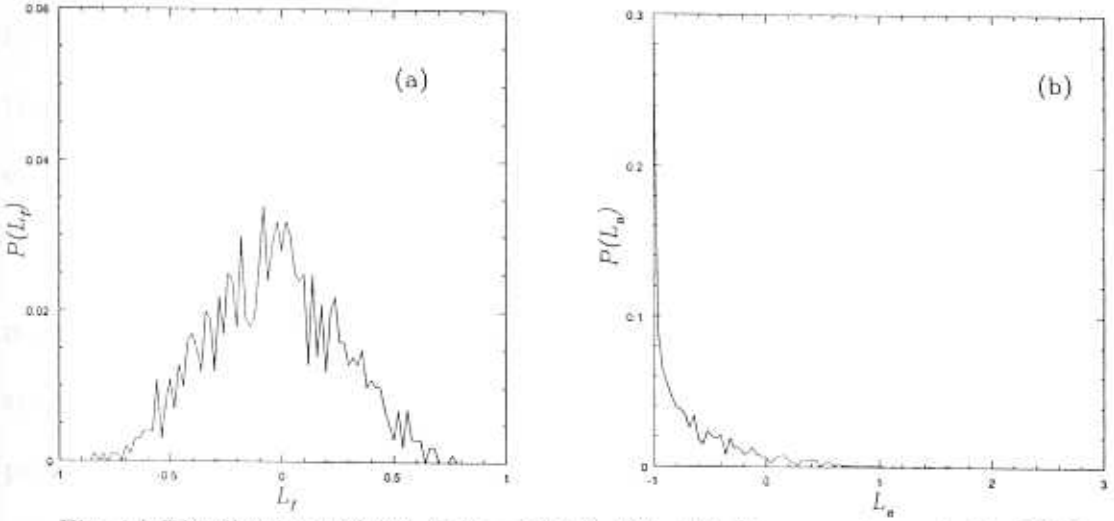

Fig. 4.9 Distribution of (a) $L_f(\vec{n})$ and (b) $L_a(\vec{n})$ at high temperatures in the $SO(3)$ theory for the $\langle L_a \rangle$ negative state. This is on a 7^3 3 lattice with $\beta_a = 3.5$.

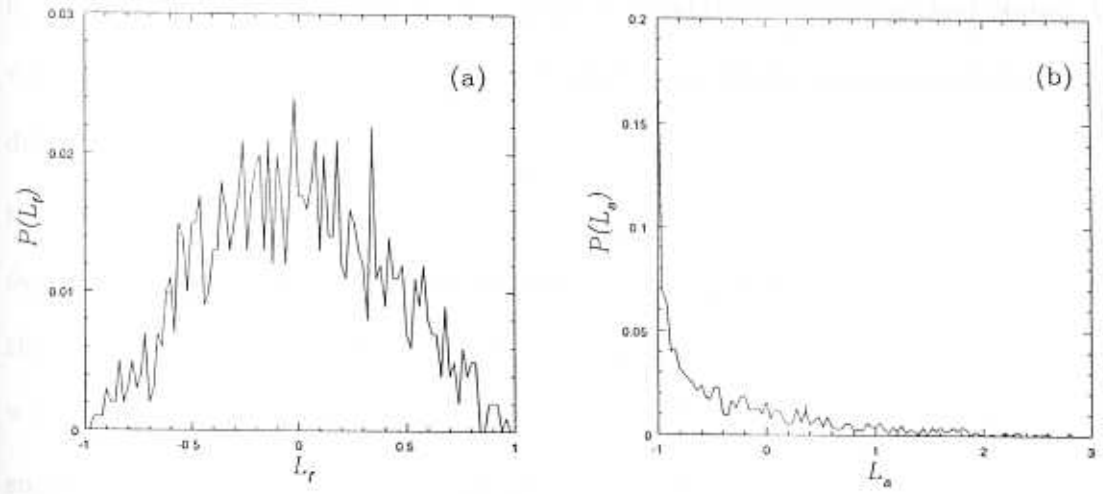

Fig. 4.10 Distribution of (a) $L_f(\vec{n})$ and (b) $L_a(\vec{n})$ in the $SO(3)$ theory on a symmetric 7^4 lattice at $\beta_a = 3.5$.

state (Fig. 4.10). Note the close similarity between them and the ones for the $\langle L_a \rangle$ negative state on a asymmetric lattice (compare Fig. 4.9 and Fig. 4.10). Thus the $\langle L_a \rangle$ negative state seen on asymmetric lattices (e.g 7^3 3 in Fig. 4.1a) is the bulk

phase at non zero temperature. Since the energies of the $\langle L_a \rangle$ positive and $\langle L_a \rangle$ negative states are almost equal, we see both these states in simulations. This is the reason why we see the bulk phase even on asymmetric lattices. Also, on asymmetric lattices we observe only the state with $\langle L_a \rangle$ positive appearing immediately after the transition, while the state with $\langle L_a \rangle$ negative starts appearing only at larger values of β_a.

As we remarked earlier, the state with $\langle L_a \rangle$ positive has a lower energy on asymmetric lattices and corresponds to the true ground state. On the other hand, on symmetric lattices, we never see the state with $\langle L_a \rangle$ positive and the system always prefers the $\langle L_a \rangle$ negative state (for a hot start). The inability of the cold start to settle into the $\langle L_a \rangle$ negative state on a symmetric lattice (see Fig. 4.8b), may be due to its correlated nature. It seems to be causing some kind of tunnelling behaviour between the bulk ($\langle L_a \rangle$ negative) and finite temperature ($\langle L_a \rangle$ positive) states. We will have more to say about this behaviour shortly. We have measured the energy difference between the $\langle L_a \rangle$ negative and $\langle L_a \rangle$ positive states, as a function of temperature. This was done by fixing β_a and varying N_τ. Two values of β_a, $\beta_a = 3.0$ and $\beta_a = 5.0$ were chosen. As N_τ is decreased (increasing temperature), we notice that the energy difference between the $\langle L_a \rangle$ positive and $\langle L_a \rangle$ negative states increases with temperature. The energy of the state with $\langle L_a \rangle$ positive becomes smaller and smaller than that of the $\langle L_a \rangle$ negative state. This difference is strikingly brought out at $\beta_a = 5.0$ (Fig. 4.11). On the symmetric lattice ($N_\tau = N_\sigma$), there is only the $\langle L_a \rangle$ negative state, while the $\langle L_a \rangle$ positive state starts appearing at some $N_\tau < N_\sigma$ (non zero temperature). We have not been able to locate the precise value at which the high temperature phase appears, because even on a 7^3 6 lattice (very low temperature), the state with $\langle L_a \rangle$ positive has a lower energy than the $\langle L_a \rangle$ negative

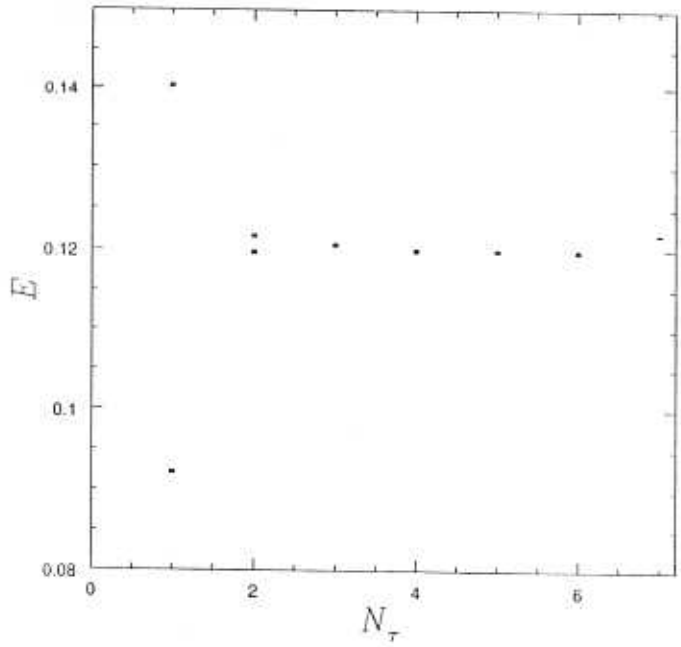

Fig. 4.11 The energies of the $\langle L_a \rangle$ positive (solid points) and $\langle L_a \rangle$ negative (open points) states as a function of N_τ for $\beta_a = 5.0$. The $\langle L_a \rangle$ positive states have a lower energy.

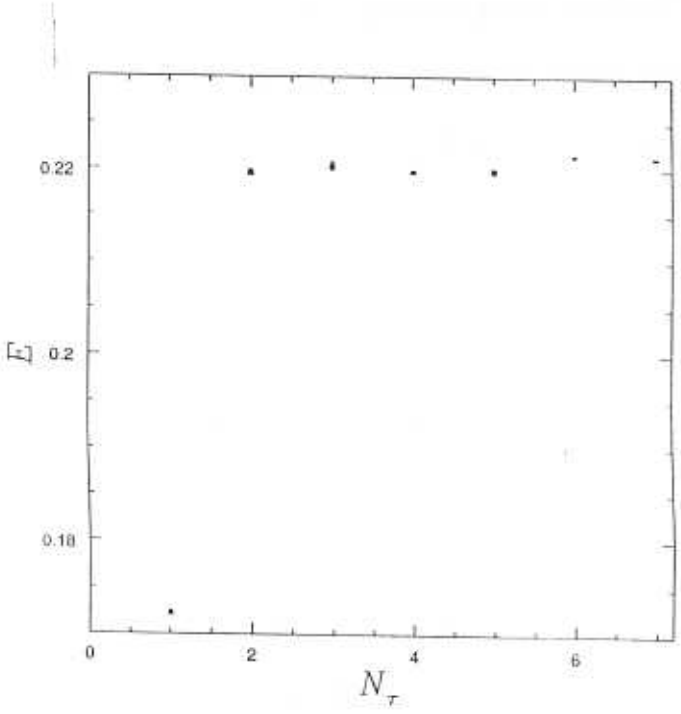

Fig. 4.12 The energies of the $\langle L_a \rangle$ positive (solid points) and $\langle L_a \rangle$ negative (open points) states as a function of N_τ for $\beta_a = 3.0$. The $\langle L_a \rangle$ positive states have a lower energy.

state. Note that there is only the $\langle L_a \rangle$ negative state on the 7^3 lattice. For $\beta_a = 3.0$, we again see the lowering in energy of the $\langle L_a \rangle$ positive state on increasing the temperature, though the difference does not decrease as much (Fig. 4.12). For this value of coupling, we do not see the $\langle L_a \rangle$ positive state at $N_\tau = 6$ as we did for $\beta_a = 5.0$. The $\langle L_a \rangle$ positive state starts appearing only at $N_\tau = 5$ and has a lower energy than the $\langle L_a \rangle$ negative state. Also, at $N_\tau = 1$ (very high temperature) there is only the $\langle L_a \rangle$ positive state. From the above observations, we conclude that the transition is from the low temperature confining phase ($\langle L_a \rangle$ negative) to the high temperature deconfining phase ($\langle L_a \rangle$ positive), at a temperature which is very small on the lattices and couplings we are using. Moreover, the value of the critical temperature though very small, seems to be slightly higher for $\beta_a = 3.0$ than for $\beta_a = 5.0$. Since the critical temperature is likely to be higher at smaller values of β_a, we have considered $\beta_a = 2.7$, which is very close to the transition point on the 7^3 3 lattice. For this coupling, the phase with $\langle L_a \rangle$ positive still does not appear for $N_\tau = 6$. We show in Fig. 4.13b, the histogram for L_a on this lattice. This was got after studying the configurations from a cold start. Note the double peak structure in this histogram. The peak at positive values of L_a is higher than the one at negative values. There is also a significant density at $L_a \approx 0$. The single site histogram for $L_f(\vec{n})$ (Fig. 4.13a) is also shown. The single peak centered about zero as in Fig. 4.10a is also seen to be breaking up into two peaks. Such double peaks are often seen in the phase coexistence region of first order phase transitions. The energy density on the other hand does not show a double peak structure. We show similar histograms for $N_\tau = 5$ at $\beta_a = 2.7$ (Fig. 4.14). Here the double peaks have weakened and the system is spending much more time in the $\langle L_a \rangle$ positive phase. We also present the single site histograms for $L_a(\vec{n})$ on the $N_\tau = 6$ and $N_\tau = 5$ lattices (Fig. 4.15).

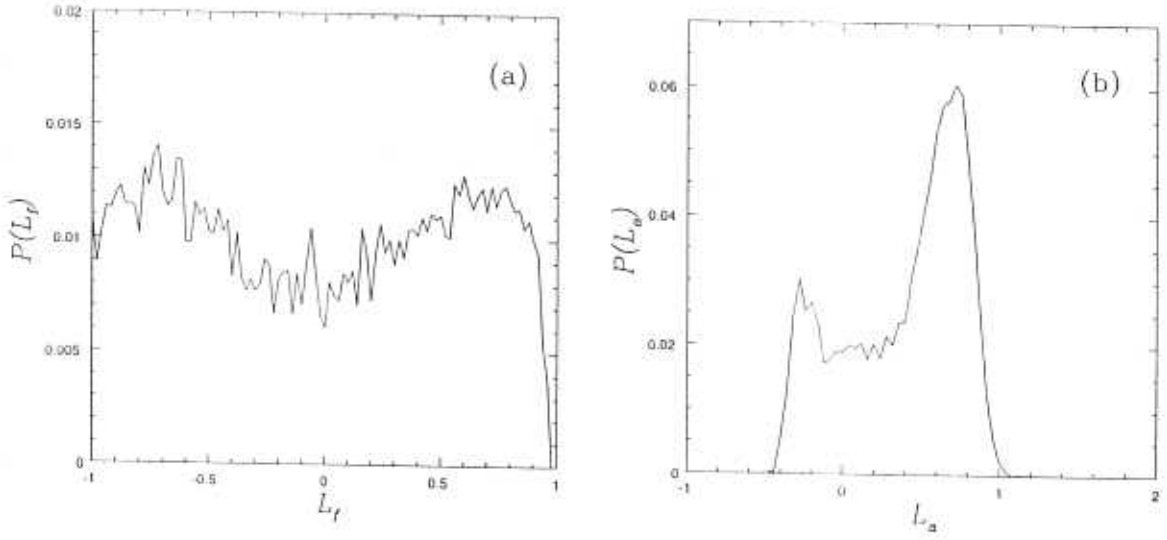

Fig. 4.13 Distribution of (a) $L_f(\vec{n})$ and (b) L_a on a 7^3 6 lattice for $\beta_a = 2.7$.

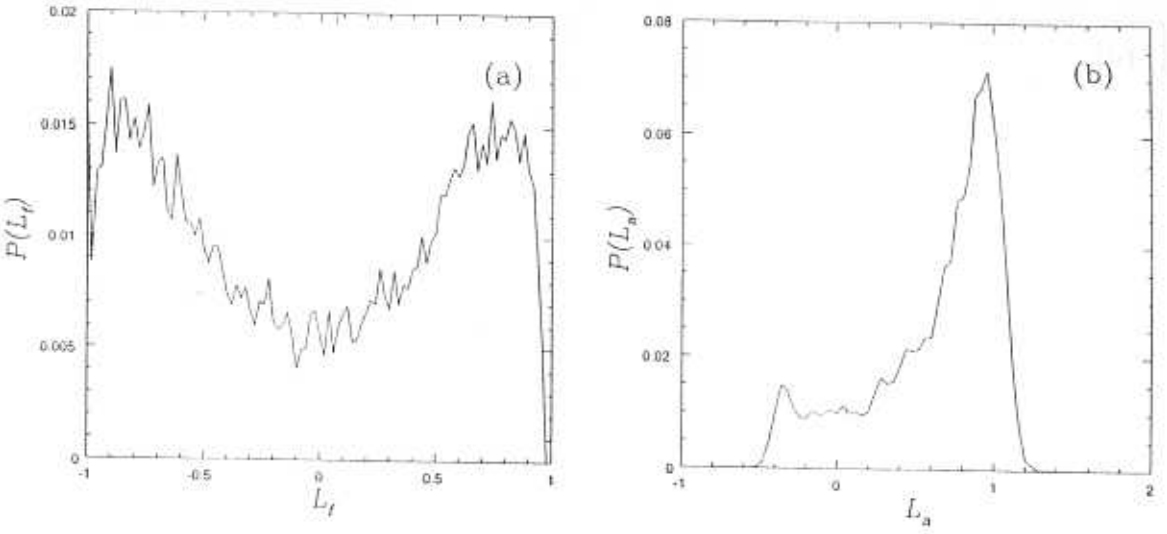

Fig. 4.14 Distribution of (a) $L_f(\vec{n})$ and (b) L_a on a 7^3 5 lattice for $\beta_a = 2.7$.

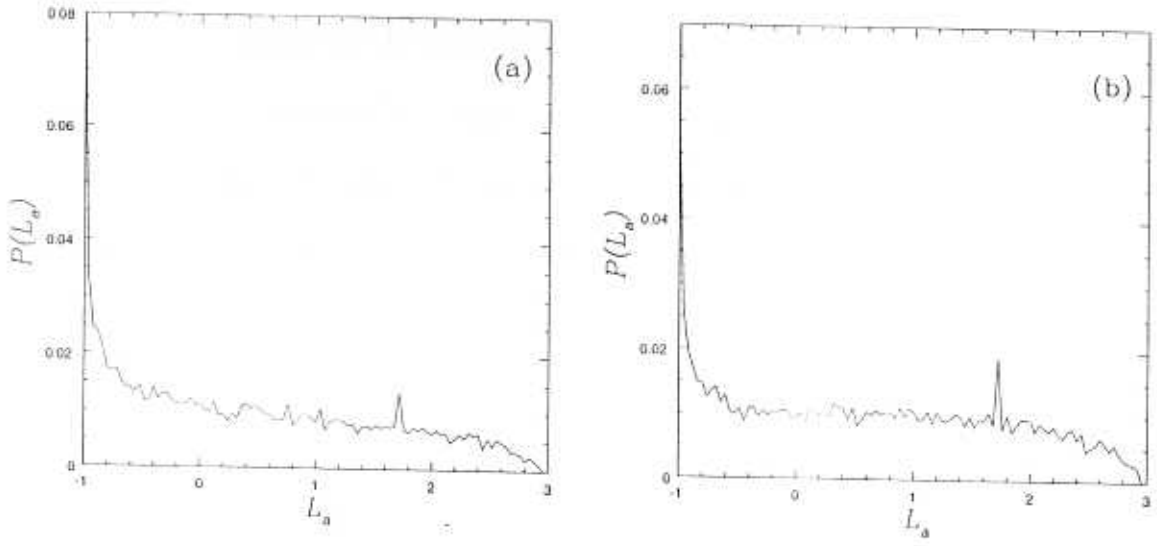

Fig. 4.15 Distribution of $L_a(\vec{n})$ for (a) $N_\tau = 6$ and (b) $N_\tau = 5$, for $\beta_a = 2.7$.

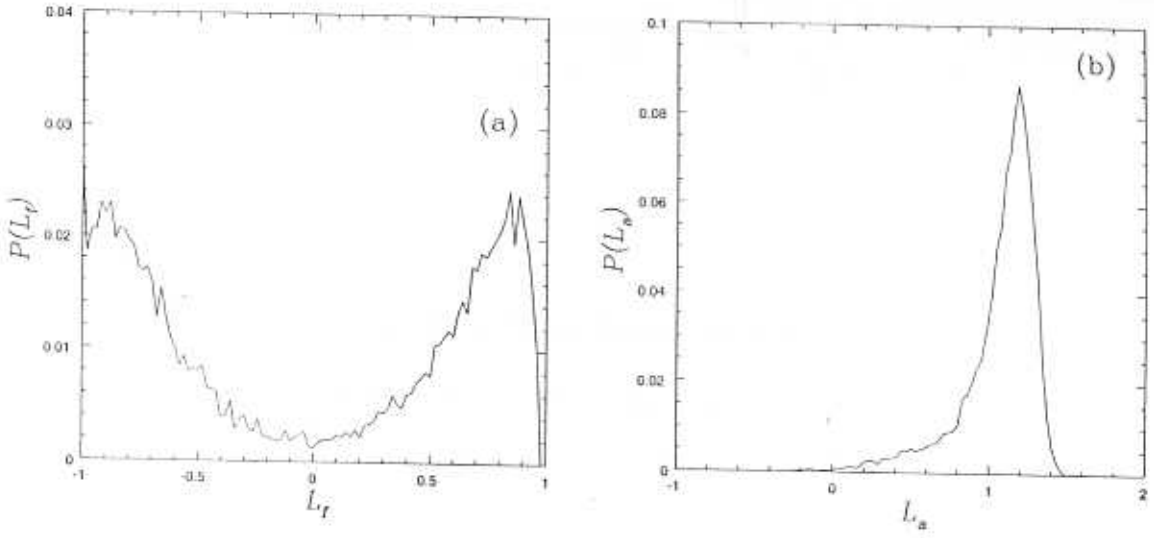

Fig. 4.16 Distribution of (a) $L_f(\vec{n})$ and (b) L_a on $N_\tau = 4$ lattice for $\beta_a = 2.7$.

Note the slight change in the distribution of $L_a(\vec{n})$ on these two lattices. On the $N_\tau = 4$ lattice, the system has completely moved into the $\langle L_a \rangle$ positive phase and the histograms show a single phase structure (Fig. 4.16 and Fig. 4.17). All the above mentioned histograms were obtained after performing 100000 Monte-Carlo sweeps. We interpret these histograms as arising out of tunnelling of configurations between

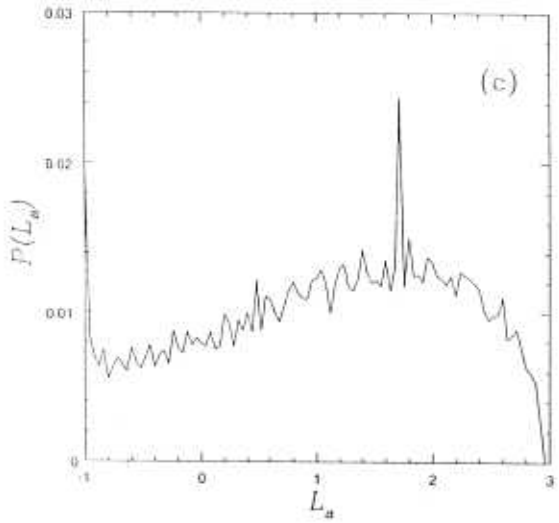

Fig. 4.17 Distribution of $L_a(\vec{n})$ for the $N_\tau = 4$ lattice at $\beta_a = 2.7$.

the $\langle L_a \rangle$ negative and $\langle L_a \rangle$ positive states. This is because we are somewhere near, if not exactly at the transition temperature. We offer this as further evidence for the existence of a transition at very low temperature.

Let us briefly summarize what we have done. For large values of β_a, we observed a transition from a bulk phase (the state with $\langle L_a \rangle$ negative on a symmetric lattice) to a high temperature phase (the state with $\langle L_a \rangle$ positive on a asymmetric lattice). We were unable to locate the transition precisely on the lattices that we were using. This is because by varying N_τ we change the temperature only in discrete steps. Across

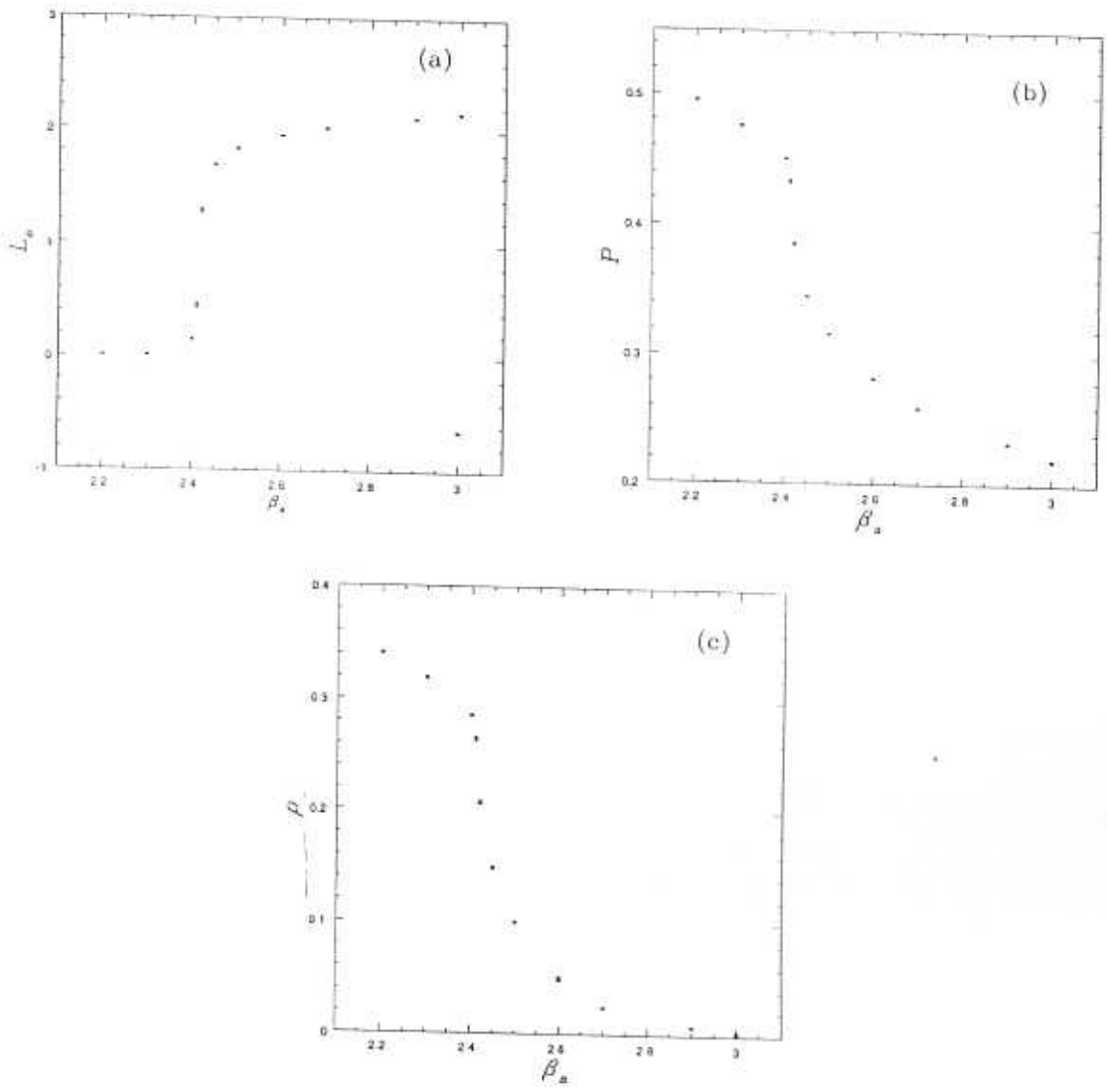

Fig. 4.18 The behaviour of (a) $\langle L_a \rangle$, (b) Energy density (P) and (c) $Z(2)$ monopole density on a 7^3 2 lattice.

this transition, $\langle L_a \rangle$ changed from a negative value to a positive value. Despite this discontinuous jump in $\langle L_a \rangle$, other quantities like the energy density changed quite smoothly (see Fig. 4.11 and Fig. 4.12). Since we are not even able to locate the transition with precision, we cannot make any concrete statement about its order. However, the smooth behaviour of the energy density across it suggests a weak first order transition.

At small β_a, the high temperature properties can be understood from the be-

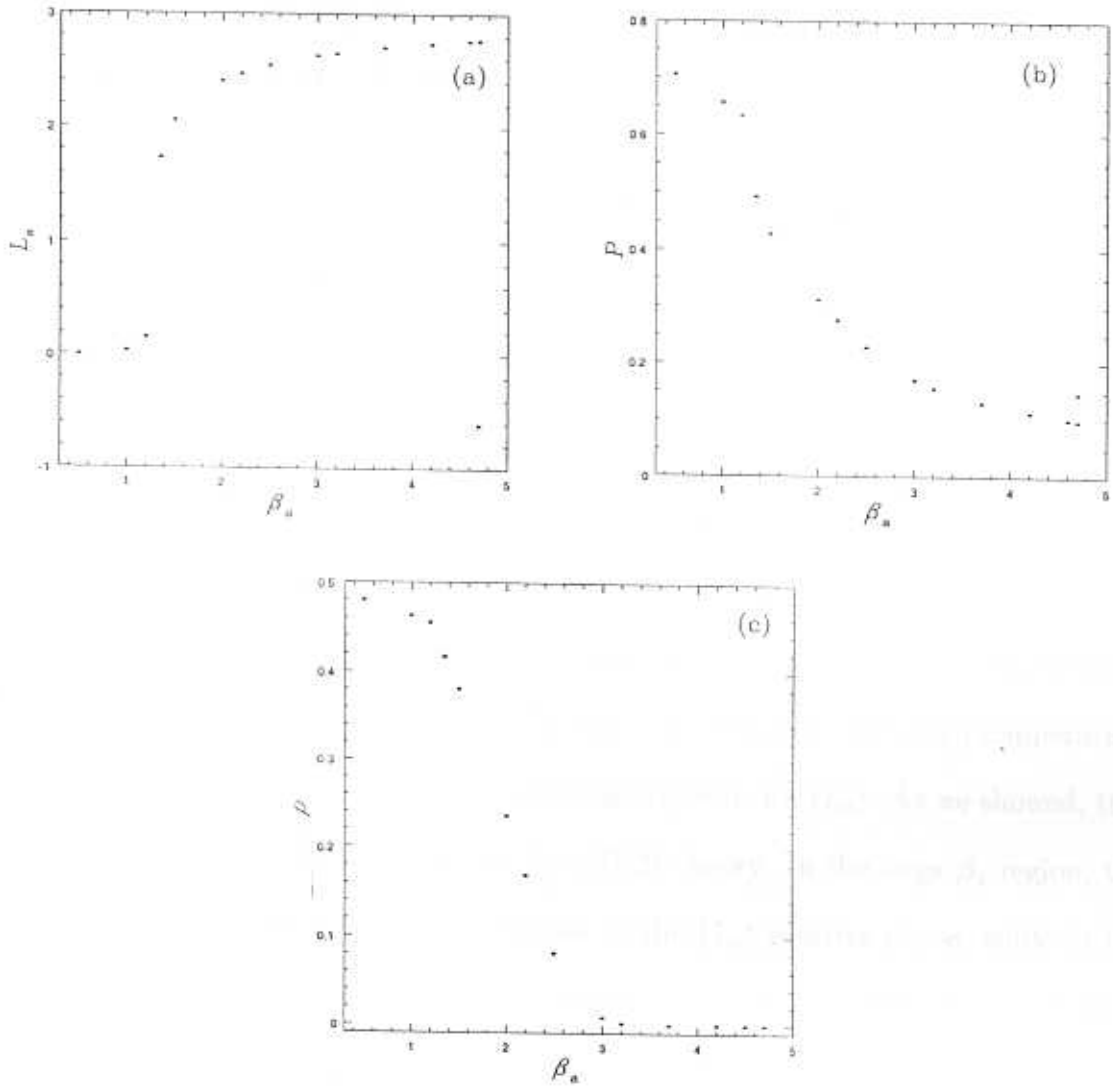

Fig. 4.19 The behaviour of (a) $\langle L_a \rangle$, (b) Energy density (P) and (c) $Z(2)$ monopole density on a 7^3 1 lattice.

haviour of the zero temperature bulk transition. We already mentioned that the $SO(3)$ LGT has a transition at zero temperature, which is driven by the decondensation of $Z(2)$ monopoles at $\beta_a \approx 2.6$. This is known to be a confinement to confinement transition. As the temperature increases, the $Z(2)$ monopoles decondense at a smaller value of β_a, due to the thermal fluctuations. The transition seen on the 7^3 3 lattice at $\beta_a \approx 2.6$ is precisely this bulk transition, though the critical β_a has not shifted much from its zero temperature value. At higher temperatures

(lattices of smaller temporal extent), the critical β_a keeps decreasing. This shift in the critical value of β_a is clearly seen by studying the monopole density or the energy density on 7^3 2 (Fig. 4.18) and 7^3 1 (Fig. 4.19) lattices. Another feature seen on these lattices is the appearance of the $\langle L_a \rangle$ negative states only at larger values of β_a. This is because these lattices correspond to higher temperatures, and a larger value of β_a is required to see the bulk phase.

Now we present our conjectured phase diagram for the $SO(3)$ LGT at finite temperature (Fig. 4.20). The small β_a phase at zero temperature is a condensate of $Z(2)$ monopoles. The large phase has a very low density of $Z(2)$ monopoles. Both these phases are confining phases. Both of them undergo transitions to a common high temperature phase, although at different temperatures. This high temperature phase is characterized by a non zero and positive value for $\langle L_a \rangle$. As we showed, this phase is like the deconfined phase of the $SU(2)$ theory. In the large β_a region, the transition is from the $\langle L_a \rangle$ negative phase to the $\langle L_a \rangle$ positive phase, while in the small β_a region, it is due to a decondensation of $Z(2)$ monopoles. In the small β_a region, we show the shift in the critical coupling causing monopole decondensation. In the large β_a region, we indicate the expected transitions by a dotted line. For large β_a, the dotted line would fall off to zero in a manner consistent with asymptotic freedom, just as in the $SU(2)$ theory. As a consequence of asymptotic freedom, this line is very flat for large β_a. At smaller β_a, it would rise and join the line of bulk transitions (shown by a solid line). The point of contact is very close to the $T = 0$ axis. This is because as we have already seen, the critical temperature is very small on the lattices we are using. An explanation for this is provided by the relation between the couplings of the $SU(2)$ and $SO(3)$ theories in the classical limit in Eq. 4.4. To see a transition in the $SO(3)$ theory for $\beta_a > 2.6$, one would have to be

in the region $\beta_f > 5.76$ of the corresponding $SU(2)$ theory. This requires lattices

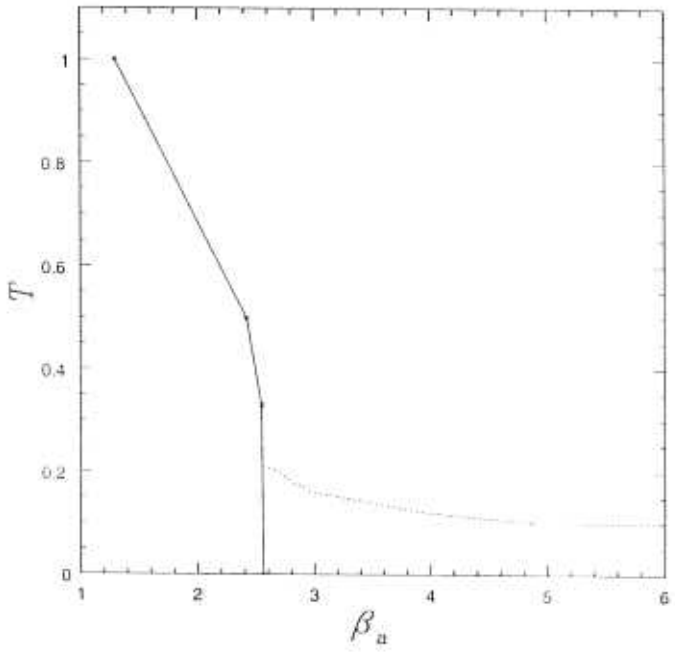

Fig. 4.20 The finite temperature phase diagram for the $SO(3)$ LGT. The solid line indicates the bulk transition while the dotted line is the finite temperature transition. Here $T = \frac{1}{N_\tau}$.

of large temporal extent. Note that $\beta_f^{cr} = 2.76$ on a $N_\tau = 16$ lattice [25], which corresponds to a very low temperature at a fixed value of β_a. The phase diagram of the $SO(3)$ LGT can be contrasted with that of the $SU(2)$ theory. In the $SU(2)$ theory, the line of finite temperature transitions rises much faster (at small β_f) than in the $SO(3)$ theory. For $N_\tau = 3$ ($T = 0.33$ in lattice units) it will be at $\beta_f = 2.2$ which is much above the line in the $SO(3)$ theory. This difference in behaviour at small β_f (β_a) in the two theories is because of the $Z(2)$ monopoles, which are copious in the $SO(3)$ theory while they are sparse in the $SU(2)$ theory.

Finally, we mention that the positivity of the free energy of an adjoint quark requires $\langle L_a \rangle$ to be always positive. But we have observed a negative value for $\langle L_a \rangle$. We suggest that as the lattice size is increased in all directions, the absolute value

of $\langle L_a \rangle$ will decrease and probably become small and positive in the thermodynamic limit.

Appendix A

In this appendix we present some details about the simulation procedure which we adopted in order to obtain our results. We used the Metropolis algorithm in generating successive Monte-Carlo configurations. A new configuration for a link variable was generated by multiplying the old link variable by an $SU(2)$ matrix, which was chosen at random from a table of 100 such elements. In order to satisfy the principle of detailed balancing, the table contained the inverse of every element present in it. This table was generated afresh after all the links in the lattice were updated once. Our simulations were usually for 10000 sweeps and measurements were made at every tenth sweep. The autocorrelation function was quite small after ten sweeps so that we could regard configurations separated by ten sweeps as independent ones. In some cases, we performed simulations upto 100000 sweeps as indicated in the appropriate places. The errors were estimated by simply calculating the square root of the variance of the data.

Appendix B

Here we show that the $SO(3)$ LGT in the strong coupling limit can be rewritten as a spin model with a local $Z(2)$ symmetry. Our calculation is performed in the Hamiltonian formalism. The calculation for the $SO(3)$ theory closely parallels that of the $SU(2)$ theory except that while calculating the trace, only integer angular momentum representations are summed over. We depart from the calculation of [7] while summing over the representations of $SU(2)$. In the $SU(2)$ theory, the contribution to the partition function at a particular link is given by

$$\sum_{j=0,1/2}^{\infty} \exp(\frac{-\beta g^2 j(j+1)}{2a}) \sin[(j+1/2)l] \sin[(j+1/2)l'] \qquad (4.19)$$

In the $SO(3)$ case, this summation has to be performed only over integral values of j. Writing the product of sine functions in terms of cosines, we get

$$\frac{1}{2}\exp(\frac{\beta g^2}{8a})\sum_{j=0}^{\infty}\exp\Big((\frac{-\beta g^2}{2a})(j+1/2)^2\Big)[\cos((j+1/2)(l-l'))-\cos((j+1/2)(l+l'))], \tag{4.20}$$

where we have also completed $j(j+1)$ to a square. Relabelling the summation by $j'=2j+1$, we get

$$\frac{1}{2}\exp(\frac{\beta g^2}{8a})\sum_{j'=1,3}^{\infty}\exp(\frac{-\beta g^2 j'^2}{8a})[\cos(j'(\frac{l-l'}{2}))-\cos(j'(\frac{l+l'}{2}))] \tag{4.21}$$

Since j takes only integer values, j' takes only odd values. In the case of $SU(2)$, the summation would have been over all values of j' since j takes all half integral values. The respective summations for $SU(2)$ and $SO(3)$ are

$$\frac{1}{2}\exp(\frac{\beta g^2}{8a})\sum_{j'=1,2}^{\infty}\exp(\frac{-\beta g^2 j'^2}{8a})[\cos(j'(\frac{l-l'}{2}))-\cos(j'(\frac{l+l'}{2}))], \tag{4.22}$$

$$\frac{1}{2}\exp(\frac{\beta g^2}{8a})\sum_{j'=1,3}^{\infty}\exp(\frac{-\beta g^2 j'^2}{8a})[\cos(j'(\frac{l-l'}{2}))-\cos(j'(\frac{l+l'}{2}))]. \tag{4.23}$$

Under the transformation $l\to 2\pi-l$ and $l'\to 2\pi-l'$, both Eq. 4.22 and Eq. 4.23 are unchanged. This is the global $Z(2)$ symmetry which is present in both models. However, only Eq. 4.23 is invariant under $l\to 2\pi-l$ and $l'\to l'$. This is because under this transformation, the terms in Eq. 4.23 just get rearranged. Eq. 4.22 is clearly not invariant under this transformation because odd j' terms are unchanged, while the even j' terms pick up an overall sign. Thus the effective spin model for the $SO(3)$ theory in the strong coupling limit has a local $Z(2)$ invariance. Using this property, the partition function for the $SO(3)$ theory can be written as

$$Z=\int_0^{2\pi}\prod_{\vec{n}}d\vec{l}(\vec{n})\sin^2\left(\frac{l(\vec{n})}{2}\right)\prod_{\vec{n}\ i}\frac{F'(l(\vec{n})+l(\vec{n}+i),l(\vec{n})-l(\vec{n}+i))}{\sin(\frac{l(\vec{n})}{2})\sin(\frac{l(\vec{n}+i)}{2})} \tag{4.24}$$

and

$$F'(l+l';l-l') = \frac{1}{2}(F(l+l';l-l') + F(2\pi - l + l'; 2\pi - l - l')) \qquad (4.25)$$

where $F(l+l';l-l')$ is the function occurring in the $SU(2)$ theory (see Chapter 2).

Chapter 5

Conclusions.

In this thesis we made a study of the $SO(3)$ LGT at finite temperature. We mainly considered the properties of the Wilson-Polyakov line defined in the adjoint representation of $SU(2)$. The behaviour of the $Z(2)$ monopole density in determining the various phases of the theory was also considered. We showed that the high temperature phase of the $SO(3)$ LGT is like the deconfined phase of the $SU(2)$ LGT. Unlike in the $SU(2)$ theory, there is no breaking of any symmetry in the high temperature phase. Since the $SU(2)$ and $SO(3)$ theories are expected to have the same continuum limit, this casts doubt on the relevance of the center symmetry for the continuum limit. Since the $SO(3)$ LGT has a zero temperature transition, we noticed an interference of the bulk phase in the finite temperature system. We were able to trace the behaviour of the bulk transition with temperature. This transition is of first order and is caused by the decondensation of $Z(2)$ monopoles, just as in the zero temperature theory. In addition, we presented evidence for a new phase transition in the large β_a region, which is the region of relevance for the continuum theory. Though we were not able to locate the transition precisely, we showed that the energy density changed smoothly across the transition. The adjoint Wilson line on the other hand, changed discontinuously across the transition. Based on this behaviour, we suggested that the transition was weakly of first order. Since a second order transition is required to take the continuum limit we suggest that this

transition will weaken as we approach the continuum limit. We then presented our conjectured phase diagram for the $SO(3)$ LGT at finite temperature. We would now like to discuss some of the implications of our results for the high temperature phase of the $SU(2)$ Yang-Mills theory. The single site histograms for $L_a(\vec{n})$ show that the configurations in the high temperature phase are mainly clustered around positive values of $L_a(\vec{n})$. Since the trace of the Wilson line in the adjoint representation can be written as $L_a(\vec{n}) = 1 + 2\cos(\theta(\vec{n}))$, this implies that $\theta(\vec{n})$ is peaking at certain values. But $\theta(\vec{n})$ is nothing but the phase of the Wilson line variable. It is the $\beta A_4(\vec{x})$ field of the continuum theory in a particular gauge. This indicates that the $A_4(\vec{x})$ field is getting a non zero expectation value in the high temperature phase. Unlike the $\theta(\vec{n})$ field, which is gauge invariant, $A_4(\vec{x})$ is not a gauge invariant observable. Hence, at high temperatures the theory is in the Higgs phase. We can define the Higgs phase in terms of a gauge invariant object like $\theta(\vec{n})$ or in terms of a gauge variant object like $A_4(\vec{x})$. Studies of the effective potential of $A_4(\vec{x})$ [33] have suggested that the $SU(2)$ Yang-Mills theory is in the Higgs phase at high temperatures. Arguments based on the dimensional reduction of the $SU(2)$ Yang-Mills theory at high temperatures into the $SU(2)$ adjoint Higgs model, have also considered the possibility of a Higgs phase at high temperatures [34]. It would be interesting to study the properties of the high temperature phase using the Higgs description. It is also important to determine the exact nature of the transition that we observed in the $SO(3)$ LGT and see how it behaves as we approach the continuum limit. We hope to address these issues in the future.

Bibliography

[1] T. H. Barnett et al, (JACEE collab.), Phys. Rev. Lett. **50**, 2062 (1983).

[2] D. Gross and F. Wilczek, Phys. Rev. Lett. **26**, 1343 (1973) ; H. Politzer, Phys. Rev. Lett. **26**, 1346 (1973).

[3] J. Collins and M. Perry, Phys. Rev. Lett. **34**, 135 (1975).

[4] A. Linde, Rep. Prog. Phys. **42**, 389 (1979).

[5] K. G. Wilson, Phys. Rev. **D10**, 2445 (1974).

[6] N. Metropolis, M. Rosenbluth, E. Teller and J. Teller, J. Chem. Phys. **21**, 1087 (1953).

[7] A. Polyakov, Phys. Lett. **72B**, 477 (1978) ; L. Susskind, Phys. Rev. **D20**, 2610 (1978).

[8] L. Mclerran and B. Svetitsky, Phys. Lett. **98B**, 195 (1981) ; J. Kuti, J. Polonyi and K. Szlachanyi, Phys. Lett. **98B**, 199 (1981) ; J. Engels, F. Karsch, H. Satz and I. Montvay, Nucl. Phys. **B205**, 545 (1982).

[9] L. Yaffe and B. Svetitsky, Nucl. Phys. **B210**[FS6], 423 (1982); L. Mclerran and B. Svetitsky, Phys. Rev. **D26**, 963 (1982).

[10] E. Tomboulis and L. Yaffe, Phys. Rev. **D29**, 78 (1984) ; E. Tomboulis and L. Yaffe, Phys. Rev. Lett. **52**, 2115 (1984); C. Borgs and E. Seiler, Nucl. Phys. **B215**[FS7], 125 (1983).

[11] D. Gross, R. D. Pisarski and L. Yaffe, Rev. Mod. Phys. **53**, 43 (1981).

[12] E. Mansousakis and J. Polonyi, Phys. Rev. Lett. **58**, 847 (1987); G. S. Bali, J. Fingberg, U. Heller, F. Karsch and K. Schilling, Phys. Rev. Lett. **71**, 3059 (1993); L. Karkkainen, P. Lacock, D. Miller, B. Petersson and T. Reisz, Phys. Lett. **312B**, 173 (1993); M. Casselle, R. Fiore, F. Gliozzi, P. Guaita and S. Vinti, Nucl. Phys. **B422**, 397 (1994).

[13] R. Gavai, M. Mathur and M. Grady, Nucl. Phys. **B423**, 123 (1994); R. V. Gavai and M. Mathur, **B448**, 399 (1995).

[14] T. Blum et al, Nucl. Phys. **B442**, 301 (1995).

[15] G. Batrouni and B. Svetitsky, Phys. Rev. Lett. **52**, 120 (1985); A. Gocksch and M.Okawa, Phys. Rev. Lett. **52**, 2205 (1984).

[16] G. Bhanot and M. Creutz, Phys. Rev. **D24**, 3212 (1981).

[17] J. Greensite and Lautrup, Phys. Rev. Lett. **47**, 9 (1988).

[18] K. Kajantie, C. Montonen and E.Pietarinen, Z. Phys. **C9**, 253 (1981); T. Celik, J. Engels and H. Satz, Phys. Lett. **125B**, 411 (1983); J. Kogut et. al, Phys. Rev. Lett **50**, 393 (1983).

[19] I. G. Halliday and A. Schwimmer, Phys. Lett. **B101**, 327 (1981); I. G. Halliday and A. Schwimmer, Phys. Lett. **B102**, 337 (1981); R. C. Brower, H. Levine and D. Kessler, Nucl. Phys. **B205**[FS5], 77 (1982).

[20] J. Kogut and L. Susskind, Phys. Rev. **D11**, 395 (1975).

[21] M. Creutz, *Quarks, gluons and lattices*, Cambridge University Press, Cambridge 1985.

[22] S. Elitzur, Phys. Rev. **D12**, 3978 (1975).

[23] J. Engels, J. Fingberg and M. Weber, Nucl. Phys. **B332**, 737 (1990) ; J. Engels, J. Fingberg and D. Miller, Nucl. Phys. **B387**, 501 (1992) ; R. Gavai, H. Satz, Phys. Lett. **B145**, 248 (1984).

[24] J. Kiskis, Phys. Rev. **D51**, 3781 (1992).

[25] J. Fingberg, U. Heller and F. Karsch, Nucl. Phys. **B392**, 493 (1993).

[26] T. Celik, J. Engels and H. Satz, Phys. Lett. **B133**, 427 (1984); R. V. Gavai, M. Lev and B. Petersson, Phys. Lett. **B140**, 397 (1984); F. Fucito, C. Rebbi and S. Solomon, Nucl. Phys. **B248**, 615 (1984); J. Polonyi, H. W. Wyld, J. B. Kogut, J. Shigemitsu and D. K. Sinclair, Phys. Rev. Lett. **53**, 644 (1984); F. Karsch and U. Heller, Nucl. Phys. **B251**[FS13], 254 (1985); J. Engels et. al., Phys. Lett. **B252**, 625 (1990).

[27] C. Borgs, Nucl. Phys. **B261**, 455 (1985).

[28] B. Svetitsky, Phys. Rep. **132**, 1 (1986).

[29] P. H. Daamgard, Phys. Lett. **B183**, 81 (1987); P. H. Daamgard, Phys. Lett. **B194**, 107 (1987); J. Fingberg et al, Phys. Lett. **B248**, 347 (1990).

[30] J. Kiskis, Phys. Rev. **D41**, 3204 (1990).

[31] M. Faber et al, Vienna preprint (1986).

[32] A. Neveu in *Recent Advances in Field Theory and Statistical Mechanics, Les Houches Proceedings 1982*, Ed. J. Zuber and R. Stora, North Holland Publishers, 1984.

[33] R. Anishetty, J.Phys. **G10**, 423, 429 (1984).

[34] P. Lacock et al, Nucl. Phys. **B369**, 501 (1992).